IMPACTS OF SUBSEQUENT FIRE ON PHYSICAL, CHEMICAL, AND BIOLOGICAL CHARACTERISTICS OF PREEXISTING PYROGENIC ORGANIC MATTER

By

Mengmeng Luo

A thesis submitted in partial fulfilment of the requirements for the degree of

Master of Science

(Agroecology and Soil Science)

At the

UNIVERSITY OF WISCONSIN-MADISON

2023

APPROVED:

Thea Whitman
Associate Professor
Department of Soil Science
DATE: 9/5/2023

Matthew Ruark
Professor
Department of Soil Science
DATE: 9/5/2023

Acknowledgement

I express sincere thanks to Dr. Thea Whitman for the mentorship and instruction over the past two years. I appreciate all the creative ideas, trust, care, encouragement, and support from all the perspectives. This whole research came out from ideas to this project, and to the proposal of my future work. Thea has been helping me with all these processes. Also, I thank the Department of Energy for the funding of this research as a part of the project "Dissection of Carbon and Nitrogen Cycling in Post-Fire Soil Environments using a Genome-Informed Experimental Community". Funding from DOE has supported me going to AGU and presenting this project for the first time.

I am so grateful to our collaborators Dr. Kara Yedinak and Keith Bourne from the Forest Products Lab, USDA Forest Service, for the help with fire parameterization using log burns and applying laboratory burns for my samples. And thanks for letting me use the powerful homogenizer to process my samples. Kara and Keith have contributed to a major part of the work in Chapter 2.

Since our studied subject and system is jack pine, without the trees we couldn't produce anything. So, I really appreciate Roger Bohringer from Wilson State Forest Nursery and Stuart Seaborne from Hancock Agricultural Research Station for the donation of trees. I also want to thank Troy Humphrey from Department of Soil Science for helping me cutting and grinding the tree branches to produce PyOM.

The help from the Whitman Lab is significant. I would like to thank our lab technician, Kelsey Kruger, who helped me in all the material preparation and problem solving. And thanks to Dr. Nayela Zeba for teaching me how to use the charcoalator. I would like to also thank all the lab members – Dana Johnson, Mia Keady, Dr. Tim Berry, Dr. Jaimie West, and Isabella Muscettola –

as well as the Freedman Lab for the advice and comments on my work during lab meetings and daily work.

I would like to thank my co-advisor Dr. Matt Ruark and committee member Dr. Monica Turner for the valuable advice during committee meetings.

I would like to thank MANRRS for the funding my attendance at the national conference; and to thank NAFSC emeritus committee and the Department of Soil Science for the funds for attending North American Forest Soil Conference. Presenting my work in the form of oral presentations really helped me improve verbal delivery skills and build up my confidence.

It was a great time to work and study in the Department of Soil Science, I would like to thank the staff and faculty for the support of all aspects. I would also like to thank the mentorship and help from other departments for my project.

I would like to give big thanks to the Agroecology cohort and Soil Science colleagues for all the intellectual exchange, great friendship, and considerate care. Also, thanks to my friends and mentors from Madison, Davis, and China for all the care and supports.

Finally, I would like to thank my parents for their unconditional love and supporting me emotionally and financially throughout all these years.

Abstract

The absence and readoption of fire after European settlement, along with increasing global temperatures caused by modern climate change, have resulted in higher fire frequency and higher fire intensity in many regions, which has led us to the age of the "Pyrocene". Pyrogenic organic matter (PyOM) produced during fires plays an important role in the carbon (C) cycle and in mitigating global warming due to its high persistence and low microbial availability, which leads to high C sequestration potential. However, despite its persistent nature, PyOM may be consumed or altered in subsequent fires. To understand the net effects of fire on the C cycle, we investigated how a subsequent fire affects the physical, chemical, and biological properties of PyOM produced during previous fire events.

Jack pine (*Pinus banksiana* Lamb.) PyOM produced at 350 °C was used to simulate preexisting PyOM typical of the Wisconsin jack pine barrens, and 0.45-0.55 mm quartz sand was used to simulate a soil matrix typical of the region. Log burns were conducted to simulate real-life fire intensities, generating two different heat flux (HF) profiles. Nine treatments with variables of HF profile (High, Low, and Control) and exposure depth (Surface, 1 cm, and 5 cm) were applied to the PyOM samples. We generated temperature profiles that were consistent across sample replicates and distinctive among treatments. We found that total mass losses for PyOM decreased with depth and increased with fire intensity – losses under High HF profile, at the surface, 1 cm, and 5 cm were 98.86%, 98.45%, and 29.19%, respectively, while under the low HF profile, those values were 93.51%, 47.22%, and 6.60%. Mean C losses closely tracked trends in mass loss and showed a linear correlation ($p < 0.05$). We also found that treatments with intermediate heat exposure (High HF + 5 cm and Low HF + 1cm) caused a significant drop in pH and increases in dissolved organic carbon (DOC), mineralized C, modelled degradable C, and modelled C

degradation rate ($p < 0.05$), compared to the unburned controls; while treatments with high heat exposure (High HF + Surface, High HF + 1cm, Low HF + Surface) showed increases in pH and decreases in total DOC and mineralized C (due to significant C loss) in the subsequent fire. These findings highlight that, despite its slow decomposition rates, PyOM is readily consumed and altered in subsequent fires, with important implications for changing fire regimes and the global C cycle.

Table of Contents

Tables & Figures

Chapter 1: Introduction - Occurrence of Subsequent Fire in the Context of Fire History and Modern Climate Change, and the Role of Soil Pyrogenic Organic Matter in Carbon Cycling

Changing fire regimes of the Anthropocene are intrinsically linked to political and cultural changes (Wagtendonk, 2007). Due to the readoption of prescribed fire after centuries of excessive fire suppression in many regions of the world and increasing temperature and drought events caused by modern climate change, fire frequency increases, and the time between subsequent fires gets shorter (Bowman et al., 2009). Subsequent fires both create new pyrogenic organic matter (PyOM) from unburned carbonaceous material and also oxidize the preexisting PyOM created from the previous fires (Tinkham et. al., 2016). As ecosystems with different fire return intervals (FRI) have different pyrogenic carbon (PyC) stocks, changes in fire frequency can affect the PyC and total carbon (C) stocks and alter C cycling. In this chapter, I will give a brief overview of fire in general, the impacts of fire on biogeochemistry, and how it affects the properties of PyOM and PyC.

Terms and definitions of fire

Fire at or below the square-meter scale (also known as “microsite” scale) is presented in the form of flame, which is controlled by fuel, heat, and oxygen (Parisien & Moritz, 2009; McGranahan & Wonkka, 2018). Fuel is usually flammable carbonaceous material, such as wood, grass, and leaf litter. Heat is produced from the ignition or existing flame. Oxygen is provided by the flow of the air. Fire at a small scale is usually characterized by physical and mechanistic properties (Parisien & Moritz, 2009), while a “fire regime” is used to characterize fires over a longer time scale and larger spatial scale, and is determined by a variety of parameters such as

spatial and temporal windows, ecosystem types, origins of ignition (Krebs et al., 2010), and consequences (Bowman et al., 2009).

Fire science studies sometimes use the terms "wildland fire" and "wildfire" interchangeably, however, the contexts of these terms are different. "Wildland" used in fire science and fire management-related topics often characterizes fire taking place in an undisturbed and uncultivated area that experiences minor anthropogenic impacts, such as forest and grassland, and is distinct from "urban" (Thompson & Calkin, 2011; Wagtendonk, 2007; McGranahan, et al., 2022). The terms are often connected with the frequently used concept, "wildland-urban interface". While "Wildfire" generally means unstructured and sometimes uncontrollable fire in the wildland (McLauchlan et al., 2020). It can be a spontaneous natural phenomenon if caused by lightning or can be caused by anthropogenic factors, like sparks or fires lit by people. Wildfire has been considered to be a hazard (Hardy, 2005; Wagtendonk, 2007) due to its damage to human infrastructure and health. The term "wildland fire" thus designates the type of location where the fire takes place. Wildland fires can be both controlled burns and unstructured fires.

Prescribed fire is the most used term to specifically describe intentional, controlled burns (McLauchlan et al., 2020). It is a type of anthropogenic fire and is usually used in the context of modern land management. Indigenous fire is used to describe prescribed fire operated by or in collaboration with Indigenous communities. Aboriginal fire is included in Indigenous fire, and the term is specifically used for the First Nations population in Australia (Nikolakis & Roberts, 2020).

Use and absence of the fire in the Anthropocene

Archeological evidence indicates that fire has been used by Indigenous people as a traditional ecological management practice in maintaining and creating natural habitats for plant food resources (Storm & Shebitz, 2006) and recreation purposes (Thompson & Calkin, 2011) over

millennia in different regions across the world. Fire activity can also be positively related to primary production, especially in tropical savannas (Bowman et al., 2009). It is now recognized that the formation of western forests and prairies in North America was heavily influenced by anthropogenic fire, not just wildfire (Kimmerer & Lake, 2001). The effects of anthropogenic fire in North America have been overlooked and misunderstood for a long time after European settlement (Nikolakis & Roberts, 2020). This is likely at least in part because the colonial culture views fire primarily as a threat to the living communities and timber industry (Christianson, 2014; Hardy, 2005).

Starting from the 17th century, Indigenous anthropogenic fire drastically decreased and essentially disappeared from the East by the early 1700s and from the West by the end of the 1800s (Guyette et al., 2002; Kimmerer & Lake, 2001). In the early 1900s, the Forest Service was established mainly for the purpose of fire suppression, until the 1970s, when the policy changed and fire management finally became an alternative solution to fire control (Wagtendonk, 2007; Williams et al., 2012). From the absence of fire in the last centuries, many fire-dependent landscapes, such as oak savanna and tallgrass prairie, have been entirely altered (Kimmerer & Lake, 2001) in the form of landscape homogeneity, dense landcover, and landscape reconstruction, such as conversion to farmland or urban land as the outcome of industry development (Guyette et al., 2002; Ryan et al., 2013). The change in the landscape also led to the change in fire regimes across major areas of the United States (Ryan et al., 2013).

Thus, wildfire frequency decreased sharply in North America during the past centuries, which is, in turn, related to the increase in the potential for fire occurrence and fire severity in the current era. Long-time absence of fire can increase the abundance of fire-sensitive plant species,

fuel continuity, homogeneity of the landscape, and number of dead trees, which can lead to the accumulation of hazardous fuels and increase the risk of more severe wildfires (Ryan et al., 2013).

Fire in the modern era

Today, as people become more and more aware of the consequences of the past excessive fire suppression and the importance of ecological restoration, prescribed fire has been reintroduced to many ecosystems as a useful landscape management tool. It can eradicate invasive species, assist in seed germination of desirable species, enhance biodiversity, and create wildlife habitats without causing severe negative effects when frequently used (Xu et al., 2022). Relatively short-interval reburns can be used as a sustainable management tool for sites with similar historical fire regimes before the exclusion of Indigenous people (Saberi & Harvey, 2023). Because reintroducing fire to a landscape with long-term absence of fire will not necessarily remove all the hazardous fuels, a second burn is often necessary for more effective fuel removal and restoring the landscape to the pre-settlement ecosystem (Lutz et al., 2020). In addition to management-related effects on fire regimes, climate change is exacerbating the risk of wildfire events in many regions of North America, due to increasing temperatures, extending warm seasons, drought events, and pest infestations (Mansoor et. al. 2022; Westerling et. al. 2006). Together, the result of these changing drivers of fire is that wildfires in many regions of North America may occur at a relatively higher frequency than in the past several centuries. Anthropogenic fire can be used to buffer climate influences on fire activity and behavior, and this buffering effect is strongest at the local scale in reducing surface fuel continuity, creating patchy burning, and retaining fuels for subsequent burns (Roos et al., 2022). Whether operating in the context of wildfire or prescribed fire, both can result in repeated burns on the same parcel of land, so subsequent fire is an important phenomenon to study.

How fire affects biogeochemical parameters

Fire can be considered as a soil forming factor when interacting with other factors, such as climate, organisms, and topography (Certini, 2013) because fire regulates C and nutrient cycles, soil microbial communities, ecological functions and interactions (McLauchlan et al., 2020), while its impact is heterogeneous at all spatial and temporal scales. Fire can create organic-rich topsoil from the combustion of plant materials, which also prone to loss when the combustion is at ground level or at high temperature and long duration (Certini et al, 2021). High heat flux and temperature from fire can also cause mortality of the soil biota directly, and also limit the resources for the organisms and microorganisms to survive (Certini et al, 2021; Whitman et al., 2019), which in return alters the landscape cover, hydrology, and the nearby watershed (Hart et al., 2005; Martin & Moody et al., 2001).

Based on the meta-analysis by Nave et al. (2011), temperate forest fires can reduce soil C and soil N through combustion by an average of 26% and 22% respectively, which can take more than 100 years to recover. The reduction in soil C and nitrogen (N) and the change in C properties vary among different ecosystems. Over longer timescales, net C and N losses from fires (elevated fire frequency compared to fire-excluded plots) occur in broadleaf forests and savanna grass, but not in needleleaf forests (Pellegrini et al., 2018). These results are interesting, particularly given that boreal forest soils hold the most C across all ecosystems (Zhang & Biswas, 2017). However, significant short-term losses of soil C and N have still been observed on the forest floor and surface mineral horizons under all studied fire intensities (Zhang & Biswas, 2017). Low-intensity ground fire can cause more soil organic matter (SOM) loss than high-intensity crown fire due to long residence of time and extensive heating (Mayer et al., 2020), while SOM in subsurface mineral horizons (<15 cm) often mostly remains intact (Zhang & Biswas, 2017). With higher fire

frequency, net losses of C and N and C:N ratio increase (Williams et al., 2012), and the loss of inorganic N can slow down the decomposition of SOM (Pellegrini et al., 2021). Although repeated fires often reduce soil C, mineral-associated C can remain protected, and the C pool that persists is often more difficult for microbes to decompose (Mayer et al., 2020; Pellegrini et al., 2021).

In contrast to the general decreases in C and N, the concentrations of phosphorous (P), calcium (Ca), magnesium (Mg), and potassium (K) can be increased by fire (Pellegrini et al., 2018) due to their higher volatilization temperatures and ash deposition (Knicker, 2007). However, much of these fire-deposited nutrients may not be obtained by plants during landscape regeneration because the basic cations may not effectively percolate into the soil due to post-fire hydrophobicity (Zhang & Biswas, 2017). Therefore, although ash produced from the fire can cause pH to increase in topsoil (Matosziuk et al., 2020; Xu et al., 2022), it may only be a temporary effect due to post-fire erosion. Besides these abiotic components, fire can also significantly decrease total microbial biomass (Mayer et al., 2020; Pressler et al., 2018), but enhance the survival of positive fire responders with higher temperature tolerance, higher reproduction rate, and preferences of the post-fire resources from the production of PyOM and PyC (Whitman et al., 2019), while this also potentially decreases microbial diversity (Pressler et al., 2018).

In contrast to general organic matter losses, we could observe a net increase in PyOM and PyC after a fire from the production of charred woods and litter, which seems to be the opposite of the typical organic matter consumption effects of fire. However, fire also consumes preexisting PyOM and PyC at the same time. Therefore, focusing on how the second fire affects the preexisting PyOM and PyC produced from the first fire is essential to understanding the net effect of fire on soil biogeochemistry.

PyOM and PyC in the biogeochemical cycle

PyOM and PyC can be found in atmospheric, aquatic, and terrestrial systems (Bird et al., 2015; Matosziuk et al., 2020, Zimmerman & Mitra, 2017). PyOM generally refers to the blackened solid residue modified from incomplete combustion (Bartoli et al., 2021; Keiluweit et al., 2010) of carbonaceous material such as leaf litter or tree branches. PyOM can be produced naturally in a fire or intentionally as "biochar". PyC is the C fraction of PyOM (Santín et al., 2016, Zimmerman & Mitra, 2017). PyC created from burns represents a large C sink globally, and soil PyC comprises the second largest PyC pool on the global scale, following the PyC in marine sediments (Bird et al., 2015; Santín et. al., 2016). Soil PyC also comprises a substantial portion of the total soil organic carbon (SOC) (Reisser et. al., 2016) and can be deposited deep in the soil profile in some ecosystems (Santín et al., 2016).

The mechanisms governing the persistence of PyOM are multifaceted. First, its elemental composition and chemical structure are largely determined by the temperature of the pyrolysis reaction in the absence of oxygen – higher temperatures produce more condensed and chemically recalcitrant aromatic structures that are supposed to be more resistant to environmental degradation (Matosziuk et al., 2019). However, PyOM is chemically heterogeneous (Keiluweit et al., 2010). For example, more aged PyOM (which is high in chemical recalcitrance) can generate more dissolved aromatic C than newly produced PyOM (Abiven et al., 2011); despite high aromaticity, the water-extractable portion of the PyOM can still be highly mineralizable by microbes (Zeba et al., 2023). Furthermore, its aromatic structure cannot protect PyOM from re-combustion in an oxygen-rich environment like charcoal being used as a fuel. Besides the chemical structure of PyOM, physical protection and limited accessibility to microbial decomposition can also prevent PyOM from re-combustion and degradation. Considering the PyOM *in situ*, the burial of PyOM

can reduce its loss from the re-combustion in a subsequent fire through insulation from heat (Tinkham et al., 2016). As with all organic matter, the amount of PyC in soil decreases with soil depth but there is a preferential trend for PyC to be transferred downward over other kinds of SOC (Soucémarianadin et al., 2019). Also, post-fire water and wind erosion can transport PyOM from its original location and deposit or bury it in an anoxic environment (Baldock & Smernik, 2002), where the drivers of decomposition, such as microbes and enzymes, cannot access it (Abney & Berhe, 2018). This burial effect created by loess can last for millions of years and create a persistent PyC layer meters below the soil surface (Marín-Spiotta et al., 2014). So, from a geological timescale, PyC can become more persistent over time and eventually much less bio-available than other non-charred organic matter (DeLuca & Aplet, 2008).

Despite this emerging understanding, studies of the vertical distribution of buried PyC are still limited and lack quantification, as the ability for PyC to translocate and stabilize in the soil varies at both ecosystem and landscape levels. In a meta-analysis, Reisser et al. (2016) found that, on average, agricultural soils have the highest PyC fraction relative to total SOC (a mean of ~16%), followed by peatland (~12.3%), grassland (~12.1%), urban land (~10.8), then forest (~9.7%). Soil PyC storage of coniferous forests in the southern US can be as low as 5-7%, while the soil PyC storage of the boreal forest is still unquantified (Bird et al., 2015). Most soil PyC is concentrated in the smallest size fractions (<53μm) (Ansley et al., 2006), where they might be subject to translocation in soil. Theoretically, finer, older, and more aromatic PyC can be found at deeper soil profiles from water percolation (Hobley 2019; Soucémarianadin et al., 2019); however, fire-induced soil hydrophobicity can inhibit this process (Huffman et al., 2001) and PyC can be eroded, which remains as an unquantified component in the global PyC cycle (Santín et al., 2016).

In addition to the spatial distribution of PyC, the potential role of PyC in C sequestration is also controversial, particularly with respect to its turnover time. Compared with unburned woody material, PyOM has a longer turnover time and a much slower decomposition rate, partially due to the physical protection from soil aggregates and mineral association (Marschner et al., 2008). Moreover, O:C ratio determines the half-life of PyOM – the smaller the O:C ratio, the longer the turnover time. < 0.2 in O:C ratio (e.g., soot) can result in 1000 years of turnover time (Spokas, 2010). The turnover time of PyC is typically estimated to range from centuries to millennia due to its different persistence in the environment (Abney & Berhe, 2018; Bird et al., 2015; Reisser et. al., 2016), while this estimation is largely variable and has drastically decreased since the late 1990s (Abney & Berhe, 2018). Modern climate change may be related to the decrease in PyC turnover time because soil warming can lead to substantial subsoil PyC loss (Zosso, et al., 2023). Furthermore, as is the focus of this thesis, fires and changing fire regimes will likely affect PyC stocks.

The influence of fire regime on soil PyOM and PyC

Long FRI of decades to centuries can protect the preexisting PyC from being combusted in the subsequent fire and assist it percolating into the deeper soil profile or exiting from the system by erosion (Bird et al., 2015). In ecosystems with short FRI, pre-existing PyC will be more likely to be combusted in subsequent fires, as it remains vulnerable closer to the soil surface, but new PyC created from burning the fuel can be added to the system and increase the PyC stock (Tinkham et. al., 2016). These trends may be reflected in the high soil PyC storage of grassland and savanna, which have relatively frequent fires. The physical and chemical properties of PyC produced from grass may make it easier to get deposited into the soil matrix and be protected, and shorter fire residence times may make less residual PyC be combusted in the fire. Certain types of forest fires

offer a contrast – because they usually generate more heat and have longer residence times during which the residual PyC may be combusted, due to higher fuel loads and continuity. In these cases, when reintroducing fire to the ecosystem, it would be important to know the original fire regime and the fire history of the land to optimize the C sequestration potential.

In this thesis, our ecosystem of interest is the southern part of the northwestern pine barrens in Wisconsin where the serotiny level is lower than 24%, which is different than the typical boreal pine barrens with stand-replacing fires (Radeloff et al., 2004). We used jack pine (*Pinus banksiana* Lamb.) for producing PyOM samples and fire simulations. Since we obtained our trees for the experiments a lot more south of the Northwestern pine barren from managed properties instead of wildland, a relatively low-intensity, high-frequency fire regime is expected, with the comparison of other jack pine barrens in the boreal region.

Conclusion

It is important to have a historical perspective when solving ecological problems or approaching ecosystem restoration. The natural occurrence of fire and the long history of anthropogenic fire management have created many different fire-dependent ecosystems, where fire might be seen more as an ecological process and not simply as a hazard. Fire frequency has decreased in many regions of the US due to the settlement and fire suppression policies before the end of the 1900s, but the fire regime of some areas has been planned to be restored to pre-settlement conditions in recent years. Simultaneously, due to the hotter and drier climate, as well as excessively accumulated fuels, we still expect to see high-severity and frequent wildfires in many areas in the near future. Changes to fire regimes likely affects production and consumption of PyC, which represents a large C pool. Between fires, PyC can be retained *in situ* on the soil surface, buried and percolated into the deeper soil profile, transformed, and translocated out of the

ecosystem. For this study, we are interested in the PyOM and PyC that remain in the location where they have been deposited and are subjected to be reburned (Figure 1.1). We were curious about the question: what will happen to PyOM during and after the second fire? Although characterized by a chemically stable aromatic structure, PyC can also be susceptible to combustion during subsequent fires. This thesis investigates the net effect of fire by exploring how the subsequent fire affects preexisting PyOM (Figure 1.1), using methods of laboratory burns.

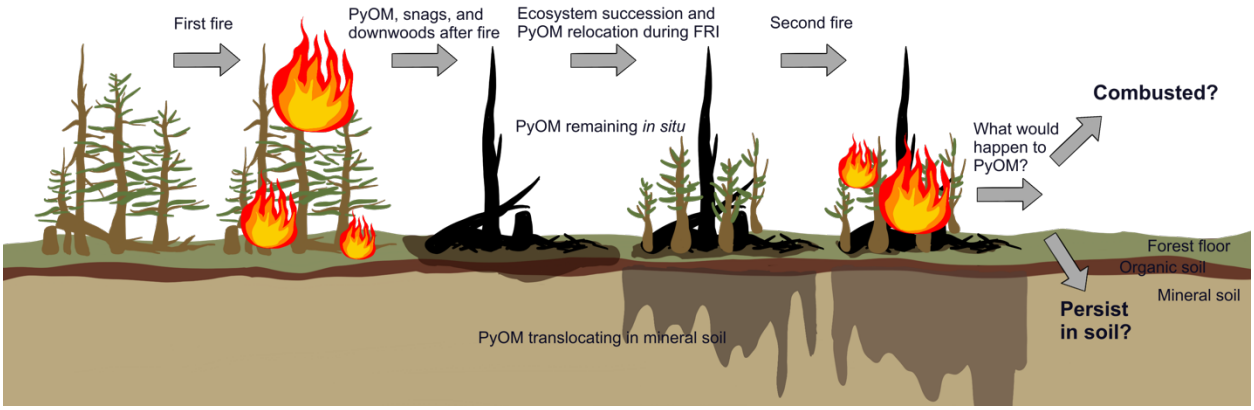

Figure 1.1. Conceptual diagram illustrating our general research question: what will happen to PyOM during and after the second fire? After the first fire, the residual PyOM on the forest floor and in organic soil decreases due to translocation and microbial degradation. Also, some PyOM percolates into mineral soil with water and biological activity and is deposited deeper in the soil profile (Santín et al., 2016; Bird et. al., 2015; Major et al., 2010). Diagram drew inspiration from Fig. 2 in Santín et al. (2016).

Reference

Abiven, S., Hengartner, P., Schneider, M. P. W., Singh, N., & Schmidt, M. W. I. (2011). Pyrogenic carbon soluble fraction is larger and more aromatic in aged charcoal than in fresh charcoal. *Soil Biology and Biochemistry*, *43*(7), 1615–1617. doi: 10.1016/j.soilbio.2011.03.027

Abney, R. B., & Berhe, A. A. (2018). Pyrogenic Carbon Erosion: Implications for Stock and Persistence of Pyrogenic Carbon in Soil. *Frontiers in Earth Science*, *6*, 26. doi: 10.3389/feart.2018.00026

Ansley, R. J., Boutton, T. W., & Skjemstad, J. O. (2006). Soil organic carbon and black carbon storage and dynamics under different fire regimes in temperate mixed-grass savanna. *Global Biogeochemical Cycles*, *20*(3). doi: 10.1029/2005gb002670

Baldock, J. A., & Smernik, R. J. (2002). Chemical composition and bioavailability of thermally altered Pinus resinosa (Red pine) wood. *Organic Geochemistry*, *33*(9), 1093–1109. doi: 10.1016/s0146-6380(02)00062-1

Bird, M. I., Wynn, J. G., Saiz, G., Wurster, C. M., & McBeath, A. (2015). The Pyrogenic Carbon Cycle. *Annual Review of Earth and Planetary Sciences*, *43*(1), 1–26. doi: 10.1146/annurev-earth-060614-105038

Bowman, D. M. J. S., Balch, J. K., Artaxo, P., Bond, W. J., Carlson, J. M., Cochrane, M. A., … Pyne, S. J. (2009). Fire in the Earth System. *Science*, *324*(5926), 481–484. doi: 10.1126/science.1163886

Certini, G. (2013). Fire as a soil-forming factor. *Ambio*, *43*(2), 191–195. doi: 10.1007/s13280-013-0418-2

Certini, G., Moya, D., Lucas-Borja, M. E., & Mastrolonardo, G. (2021). The impact of fire on soil-dwelling biota: A review. *Forest Ecology and Management*, *488*, 118989. doi: 10.1016/j.foreco.2021.118989

Christianson, A. (2014). Social science research on Indigenous wildfire management in the 21st century and future research needs. *International Journal of Wildland Fire*, *24*(2), 190–200. doi: 10.1071/wf13048

DeLuca, T. H., & Aplet, G. H. (2008). Charcoal and carbon storage in forest soils of the Rocky Mountain West. *Frontiers in Ecology and the Environment*, *6*(1), 18–24. doi: 10.1890/070070

Guyette, R. P., Muzika, R. M., & Dey, D. C. (2002). Dynamics of an Anthropogenic Fire Regime. *Ecosystems*, *5*(5), 472–486. doi: 10.1007/s10021-002-0115-7

Hart, S. C., DeLuca, T. H., Newman, G. S., MacKenzie, M. D., & Boyle, S. I. (2005). Post-fire vegetative dynamics as drivers of microbial community structure and function in forest soils. *Forest Ecology and Management*, *220*(1–3), 166–184. doi: 10.1016/j.foreco.2005.08.012

Hardy, C. C. (2005). Wildland fire hazard and risk: Problems, definitions, and context. *Forest Ecology and Management*, *211*(1–2), 73–82. doi: 10.1016/j.foreco.2005.01.029

Hobley, E. (2019). Vertical Distribution of Soil Pyrogenic Matter: A Review. *Pedosphere*, *29*(2), 137–149. doi: 10.1016/s1002-0160(19)60795-2

Huffman, E. L., MacDonald, L. H., & Stednick, J. D. (2001). Strength and persistence of fire-induced soil hydrophobicity under ponderosa and lodgepole pine, Colorado Front Range. *Hydrological Processes*, *15*(15), 2877–2892. doi: 10.1002/hyp.379

Keiluweit, M., Nico, P. S., Johnson, M. G., & Kleber, M. (2010). Dynamic molecular structure of plant biomass-derived black carbon (biochar). *Environmental Science & Technology*, *44*(4), 1247–1253. doi: 10.1021/es9031419

Kimmerer, R. W., & Lake, F. K. (2001). The Role of Indigenous Burning in Land Management. *Journal of Forestry*, *99*(11), 36–41. doi: 10.1093/jof/99.11.36

Knicker, H. (2007). How does fire affect the nature and stability of soil organic nitrogen and carbon? A review. *Biogeochemistry*, *85*(1), 91–118. doi: 10.1007/s10533-007-9104-4

Krebs, P., Pezzatti, G. B., Mazzoleni, S., Talbot, L. M., & Conedera, M. (2010). Fire regime: history and definition of a key concept in disturbance ecology. *Theory in Biosciences*, *129*(1), 53–69. doi: 10.1007/s12064-010-0082-z

Lutz, J. A., Struckman, S., Furniss, T. J., Cansler, C. A., Germain, S. J., Yocom, L. L., … Larson, A. J. (2020). Large-diameter trees dominate snag and surface biomass following reintroduced fire. *Ecological Processes*, *9*(1), 41. doi: 10.1186/s13717-020-00243-8

Major, J., Lehmann, J., Rondon, M., & Goodale, C. (2010). Fate of soil-applied black carbon: downward migration, leaching and soil respiration. *Global Change Biology*, *16*(4), 1366–1379. doi: 10.1111/j.1365-2486.2009.02044.x

Mansoor, S., Farooq, I., Kachroo, M. M., Mahmoud, A. E. D., Fawzy, M., Popescu, S. M., … Ahmad, P. (2022). Elevation in wildfire frequencies with respect to the climate change. *Journal of Environmental Management*, *301*, 113769. doi: 10.1016/j.jenvman.2021.113769

Marin-Spiotta, E., Chaopricha, N. T., Plante, A. F., Diefendorf, A. F., Mueller, C. W., Grandy, A. S., & Mason, J. A. (2014). Long-term stabilization of deep soil carbon by fire and burial during early Holocene climate change. *Nature Geoscience*, *7*(6), 428–432. doi: 10.1038/ngeo2169

Marschner, B., Brodowski, S., Dreves, A., Gleixner, G., Gude, A., Grootes, P. M., … Wiesenberg, G. L. B. (2008). How relevant is recalcitrance for the stabilization of organic matter in soils? *Journal of Plant Nutrition and Soil Science*, *171*(1), 91–110. doi: 10.1002/jpln.200700049

Martin, D. A., & Moody, J. A. (2001). Comparison of soil infiltration rates in burned and unburned mountainous watersheds. *Hydrological Processes*, *15*(15), 2893–2903. doi: 10.1002/hyp.380

Matosziuk, L. M., Gallo, A., Hatten, J., Bladon, K. D., Ruud, D., Bowman, M., … Weiglein, T. (2020). Short-Term Effects of Recent Fire on the Production and Translocation of Pyrogenic Carbon in Great Smoky Mountains National Park. *Frontiers in Forests and Global Change*, *3*, 6. doi: 10.3389/ffgc.2020.00006

Mayer, M., Prescott, C. E., Abaker, W. E. A., Augusto, L., Cécillon, L., Ferreira, G. W. D., … Vesterdal, L. (2020). Influence of forest management activities on soil organic carbon stocks: A knowledge synthesis. *Forest Ecology and Management*, *466*, 118127. doi: 10.1016/j.foreco.2020.118127

McGranahan, D. A., Maier, C., Gauger, R., Woodson, C., & Wonkka, C. L. (2022). The Dunn Ranch Academy: Developing Wildland Fire Literacy through Hands-on Experience with Prescribed Fire Science and Management. *Fire*, *5*(4), 121. doi: 10.3390/fire5040121

McGranahan, D. A., & Wonkka, C. L. (2018). Wildland Fire Science Literacy: Education, Creation, and Application. *Fire*, *1*(3), 52. doi: 10.3390/fire1030052

McLauchlan, K. K., Higuera, P. E., Miesel, J., Rogers, B. M., Schweitzer, J., Shuman, J. K., … Watts, A. C. (2020). Fire as a fundamental ecological process: Research advances and frontiers. *Journal of Ecology*, *108*(5), 2047–2069. doi: 10.1111/1365-2745.13403

Nave, L. E., Vance, E. D., Swanston, C. W., & Curtis, P. S. (2011). Fire effects on temperate forest soil C and N storage. *Ecological Applications*, *21*(4), 1189–1201. doi: 10.1890/10-0660.1

Nikolakis, W., & Roberts, E. (2020). Indigenous fire management: a conceptual model from literature. *Ecology and Society*, *25*(4). doi: 10.5751/es-11945-250411

Parisien, M.-A., & Moritz, M. A. (2009). Environmental controls on the distribution of wildfire at multiple spatial scales. *Ecological Monographs*, *79*(1), 127–154. doi: 10.1890/07-1289.1

Pellegrini, A. F. A., Ahlström, A., Hobbie, S. E., Reich, P. B., Nieradzik, L. P., Staver, A. C., … Jackson, R. B. (2018). Fire frequency drives decadal changes in soil carbon and nitrogen and ecosystem productivity. *Nature*, *553*(7687), 194–198. doi: 10.1038/nature24668

Pellegrini, A. F. A., Caprio, A. C., Georgiou, K., Finnegan, C., Hobbie, S. E., Hatten, J. A., & Jackson, R. B. (2021). Low-intensity frequent fires in coniferous forests transform soil organic matter in ways that may offset ecosystem carbon losses. *Global Change Biology*, *27*(16), 3810–3823. doi: 10.1111/gcb.15648

Pressler, Y., Moore, J. C., & Cotrufo, M. F. (2018). Belowground community responses to fire: meta-analysis reveals contrasting responses of soil microorganisms and mesofauna. *Oikos, 128*(3), 309-327. doi: 10.1111/oik.05738

Radeloff, V. C., Mladenoff, D. J., Guries, R. P., & Boyce, M. S. (2004). Spatial patterns of cone serotiny in Pinus banksiana in relation to fire disturbance. *Forest Ecology and Management*, *189*(1–3), 133–141. doi: 10.1016/j.foreco.2003.07.040.

Reisser, M., Purves, R. S., Schmidt, M. W. I., & Abiven, S. (2016). Pyrogenic Carbon in Soils: A Literature-Based Inventory and a Global Estimation of Its Content in Soil Organic Carbon and Stocks. *Frontiers in Earth Science*, *4*, 80. doi: 10.3389/feart.2016.00080

Roos, C. I., Guiterman, C. H., Margolis, E. Q., Swetnam, T. W., Laluk, N. C., Thompson, K. F., … Whitehair, L. (2022). Indigenous fire management and cross-scale fire-climate relationships in the Southwest United States from 1500 to 1900 CE. *Science Advances*, *8*(49), eabq3221. doi: 10.1126/sciadv.abq3221

Ryan, K. C., Knapp, E. E., & Varner, J. M. (2013). Prescribed fire in North American forests and woodlands: history, current practice, and challenges. *Frontiers in Ecology and the Environment*, *11*(s1), e15–e24. doi: 10.1890/120329

Saberi, S. J., & Harvey, B. J. (2023). What is the color when black is burned? Quantifying (re)burn severity using field and satellite remote sensing indices. *Fire Ecology*, *19*(1), 24. doi: 10.1186/s42408-023-00178-3

Santín, C., Doerr, S. H., Kane, E. S., Masiello, C. A., Ohlson, M., Rosa, J. M., … Dittmar, T. (2016). Towards a global assessment of pyrogenic carbon from vegetation fires. *Global Change Biology*, *22*(1), 76–91. doi: 10.1111/gcb.12985

Storm, L., & Shebitz, D. (2006). Evaluating the Purpose, Extent, and Ecological Restoration Applications of Indigenous Burning Practices in Southwestern Washington. *Ecological Restoration*, *24*(4), 256–268. doi: 10.3368/er.24.4.256

Soucémarianadin, L., Reisser, M., Cécillon, L., Barré, P., Nicolas, M., & Abiven, S. (2019). Pyrogenic carbon content and dynamics in top and subsoil of French forests. *Soil Biology and Biochemistry*, *133*, 12–15. doi: 10.1016/j.soilbio.2019.02.013

Tinkham, W. T., Smith, A. M. S., Higuera, P. E., Hatten, J. A., Brewer, N. W., & Doerr, S. H. (2016). Replacing time with space: using laboratory fires to explore the effects of repeated burning on black carbon degradation. *International Journal of Wildland Fire*, *25*(2), 242–248. doi: 10.1071/wf15131

Thompson, M. P., & Calkin, D. E. (2011). Uncertainty and risk in wildland fire management: A review. *Journal of Environmental Management*, *92*(8), 1895–1909. doi: 10.1016/j.jenvman.2011.03.015

Wagtendonk, J. W. van. (2007). The History and Evolution of Wildland Fire Use. *Fire Ecology*, *3*(2), 3–17. doi: 10.4996/fireecology.0302003

Westerling, A. L., Hidalgo, H. G., Cayan, D. R., & Swetnam, T. W. (2006). Warming and Earlier Spring Increase Western U.S. Forest Wildfire Activity. *Science*, *313*(5789), 940–943. doi: 10.1126/science.1128834

Whitman, T., Whitman, E., Woolet, J., Flannigan, M. D., Thompson, D. K., & Parisien, M.-A. (2019). Soil Bacterial and Fungal Response to Wildfires in the Canadian Boreal Forest Across a Burn Severity Gradient. *Soil Biology and Biochemistry*, 512798. doi: 10.1016/j.soilbio.2019.107571

Williams, R. J., Hallgren, S. W., & Wilson, G. W. T. (2012). Frequency of prescribed burning in an upland oak forest determines soil and litter properties and alters the soil microbial community. *Forest Ecology and Management*, *265*, 241–247. doi: 10.1016/j.foreco.2011.10.032

Xu, S., Eisenhauer, N., Pellegrini, A. F. A., Wang, J., Certini, G., Guerra, C. A., & Lai, D. Y. F. (2022). Fire frequency and type regulate the response of soil carbon cycling and storage to fire across soil depths and ecosystems: A meta-analysis. *Science of The Total Environment*, *825*, 153921. doi: 10.1016/j.scitotenv.2022.153921

Zeba, N., Berry, T. D., Fischer, M. S., Traxler, M. F., & Whitman, T. (2023). Soil carbon mineralization and microbial community dynamics in response to PyOM addition. doi: 10.1101/2023.06.21.545992

Zimmerman, A. R., & Mitra, S. (2017). Trial by Fire: On the Terminology and Methods Used in Pyrogenic Organic Carbon Research. *Frontiers in Earth Science*, *5*, 95. doi: 10.3389/feart.2017.00095

Zhang, Y., Biswas, A. (2017). The Effects of Forest Fire on Soil Organic Matter and Nutrients in Boreal Forests of North America: A Review. In: Rakshit, A., Abhilash, P., Singh, H., Ghosh, S. (eds) Adaptive Soil Management : From Theory to Practices. Springer, Singapore. https://doi.org/10.1007/978-981-10-3638-5_21

Zosso, C. U., Ofiti, N. O. E., Torn, M. S., Wiesenberg, G. L. B., & Schmidt, M. W. I. (2023). Rapid loss of complex polymers and pyrogenic carbon in subsoils under whole-soil warming. *Nature Geoscience*, 1–5. doi: 10.1038/s41561-023-01142-1

Chapter 2: Burning PyOM at Different Exposure Depths in A Sand Matrix Under High and Low Heat Flux – A Laboratory Method for Simulating Subsequent Fires

Introduction

Due to a variety of causes, including anthropogenic influences and natural disturbances, fire can reoccur in the same parcel of land. How the subsequent fire affects the pyrogenic organic matter (PyOM) produced in the previous fire has not been well-studied, but is an essential component of understanding the net effects of fire. Of the relatively few previous studies that have examined the impact of repeated fires or reburns on PyOM, most of them are field studies, which could be affected by many different variables, such as the weather conditions, wind direction, and heterogeneity of fire behavior. The study conducted by Santín et al. in 2013 represents one of the earliest field and lab experiments on the net effect of fire on the pre-existing PyOM (Santín et al., 2013). These past studies have generally concluded that in natural ecosystems, fire can add, consume, and transform pyrogenic C (PyC) (Doerr et. al., 2018). Constraints in typical method designs can be identified in four key aspects: 1) incomplete representation of PyOM and PyC, 2) overlooking the PyOM and PyC in mineral soil, 3) contamination from the fuel, and 4) difficulty in quantifying fire intensity.

Incomplete representation of PyOM and PyC

Prior studies have found that the particle size and shape of PyOM or PyC do not significantly affect mass loss through combustion, within the range of particle sizes studied (Santín et. al., 2013, Tinkham et. al., 2016, Bartoli et. al., 2021). However, these findings reflect the fact that the results from those studies were not based on all the portions of PyOM and PyC samples used for the experiments, as smaller size fractions of PyOM and PyC were not collected for the analysis. Small-sized PyOM and PyC, including soot and ash, are often highly persistent but are

generally too mobile and/or small to be effectively collected and analyzed (Matosziuk et. al., 2019, Ansley et al., 2006), with much of these materials being transported to the atmosphere by wind and deposited outside the system boundary. Consequently, studies including or focusing on the small-size fractions of PyOM and PyC are limited, despite the potential implications for carbon (C) sequestration.

Overlooking the PyOM and PyC buried in mineral soil

In addition to particle size, another challenge is the identification and quantification of PyC in mineral soil, due to the need to isolate it from other soil C. However, methods for isolating PyOM are typically destructive and inaccurate because the general principle is to remove labile organic matter (OM) and assume the rest is PyOM (Zimmerman & Mitra, 2017). Thermal oxidation and acid oxidation are two of the most commonly used methods. One example of thermal oxidation is CTO375, which removes OM and leaves "black carbon" by heating the samples at 375 °C in the presence of oxygen for over 20 hours (Gustafsson et al., 1996; Hatten et al., 2008). Benzenepolycarboxylic acids (BPCA) is a representative example of acid oxidation. It uses strong acids (like HCl) to dissolve the OM in soils, leaving aromatic compounds (BPCA) as chemical markers for condensed aromatic C (Brodowski et al., 2005; Matosziuk et al., 2020). Both kinds of methods link PyOM with high chemical recalcitrance, which is not fully accurate because the highly degradable portion of PyOM is ignored, and some of the measured aromatic C may not be produced from heating. In contrast, typical non-destructive methods can only identify PyC without separating it (Zimmerman & Mitra, 2017), thereby precluding direct chemical and biological analyses (such as mid-infrared spectroscopy, or MIR). As a result, most studies have focused on the PyC on the surface or in the organic horizon, but not in the mineral soil. Over time, PyC can move from the O horizon to mineral soil (Matosziuk et. al., 2020, Tinkham et al., 2016). This

vertical movement of PyOM and PyC can occur through bioturbation or translocation with water, while PyOM and PyC can also be produced at depth through the charring of roots and buried biomass *in situ* (Hobley 2019; Soucémarianadin et al., 2019). Previous studies of subsequent fires have suggested that PyC residing in deeper soil horizons can be protected from heat and combustion due to soil insulation (Doerr et al., 2018, Saiz et. al., 2014, Santín et al., 2013, Bartoli et al., 2021). However, there is a lack of comparative experiments to validate these statements, with most studies focusing on PyOM and PyC either on the surface or within the litter layer, not in the mineral soil.

Contamination from fuel

The use of a fuel bed, typically composed of woody materials, is a common method for sustaining heat during the PyOM burning process, designed to provide a realistic scenario for a forest fire. However, this method can contaminate the preexisting PyOM in the system due to the addition of new PyOM from the fuel, making it challenging to analyze the net effect of fire on the PyOM. Some studies have attempted to address this issue by wrapping the PyOM sample in a metal mesh bag to separate it from the fuel (Bartoli et al., 2021, Santín et al., 2013), but the metal can alter the heat transfer to the sample, and small particles of PyOM can still leak out from or into the mesh bag.

Unclear definition of fire intensity

Fire intensity is defined as the "energy output" of a fire and is not explicitly linked to any effects caused by fire (Keeley, 2009), although different effects on C storage in forests can be expected between high- and low-intensity fires, which could have implications for forest management. However, quantifying fire intensity, particularly in natural settings, is difficult.

Limitations in previous studies consist of three aspects. First, quantitative measurements of fire intensity can be misused or vaguely defined. Temperature has been used as an indicator for how much heat is dosed to the samples, (Santín et. al., 2013), which is not as direct and accurate as energy fluxes. Fireline intensity has also been used as a proxy for fire intensity in some studies (Doerr et. al., 2018). However, this concept cannot be easily translated to laboratory settings, as fireline intensity is commonly used for ecological field studies, prescribed fires, and fire suppression, not for laboratory experiments. Second, during laboratory settings, the simulated fires are not always based on real-world parameters. Some of them chose the values of temperature at a common difference (Santín et al., 2013), or chose random values within a certain range (Badía & Martí, 2003). Third, there are limited methods for measuring heat transfer downwards from fuel to the media beneath it.

Methodological approach and hypotheses

We sought to develop a method for simulating the effects of subsequent fire on PyOM that effectively addresses each of these limitations. We developed lab simulations of subsequent fire using a cone calorimeter with PyOM in a sand matrix, with the following characteristics: 1) All portions of PyOM after the reburn are collected and analyzed. 2) PyOM is buried at a range of depths within a sand matrix, to include the overlooked mineral soil while also ensuring that the PyOM sample is the only C input in the system. 3) Instead of applying a fuel bed to sustain the heat for the burn, we apply a precise heat flux (HF) dose using a cone calorimeter. 4) The HF profiles, representing high and low fire intensity, were drawn from the data captured from HF sensors under tree log burns to parameterize a realistic fire scenario.

We hypothesized that higher HF and shallower depths will have more PyOM mass losses. At the same HF, PyOM on the surface will be subject to more mass loss than PyOM at both 1 cm and 5 cm depths. At the same depth, high HF fire will consume more PyOM than low HF fire.

Methods

Ecosystem, site description, and overview of the experiment

Jack pine (*Pinus banksiana* Lamb.) wood is the key material used to produce the PyOM samples and parameterize realistic HF profiles for our experiments. Wisconsin is one of the states that have the most jack pine standings in the US (Rudolph & Laidly, 1990). Besides its commercial value as pulpwood and lumber, jack pine stands are also an important breeding area for native birds and can be used for recreation areas (Rudolph & Laidly, 1990). Jack pines are known for their dependence on fire to open their cones for seed release and germination (also known as "serotiny"). Its populations can be threatened by pest infestations, such as jack pine budworm (*Choristoneura pinus*) (Radeloff et. al., 2004; Rudolph & Laidly, 1990).

We designed our burn experiment to reflect the general ecosystem of the jack pine (*Pinus banksiana* Lamb.) barrens in Wisconsin, where the soil is characterized as coarse sands with low nutrients, low water holding capacity, and prone to drought (Radeloff et. al., 1999 & 2004). Based on the study by Radeloff et al. (2004) in the Northwestern Pine Barren, the stand-level serotiny gradually decreases from the north to the south. In the southmost region, jack pine standings are subject to the lowest stand-level serotiny (<24%) due to non-lethal high-frequency fire (with a 3~7-year fire return interval) and thick tree bark, which is the fire regime that is more expected to resemble our experiment. For this experiment, we used two jack pine trees that were cut down from Wilson State Forest Nursery (43.1461124, -90.6950388) and Hancock Agricultural Research Station (44.122667, -89.530740) in Wisconsin (Figure 2.1). Because the locations of the trees are

in the central south of Wisconsin and in managed land, we don't expect serotiny to necessarily occur in the tree origins.

To simulate the effects of repeated fire on PyOM, we pyrolyzed jack pine wood in the "charcoalator" (a modified muffle furnace; Güereña et al., 2015) under an anaerobic environment maintained under Argon (Ar) gas, and then burned the resulting PyOM under a cone calorimeter at the Forest Products Laboratory of USDA Forest Service in a sand matrix. We designed the fire to be representative of logs burning on the soil surface in a jack pine stand, including a higher and lower fire intensity. We directly quantified the HF transferred downwards into the soil in this system, and chose this approach to represent a scenario where the greatest heat transfer to soil might be likely to occur, thereby capturing the upper bounds of fire effects in this system.

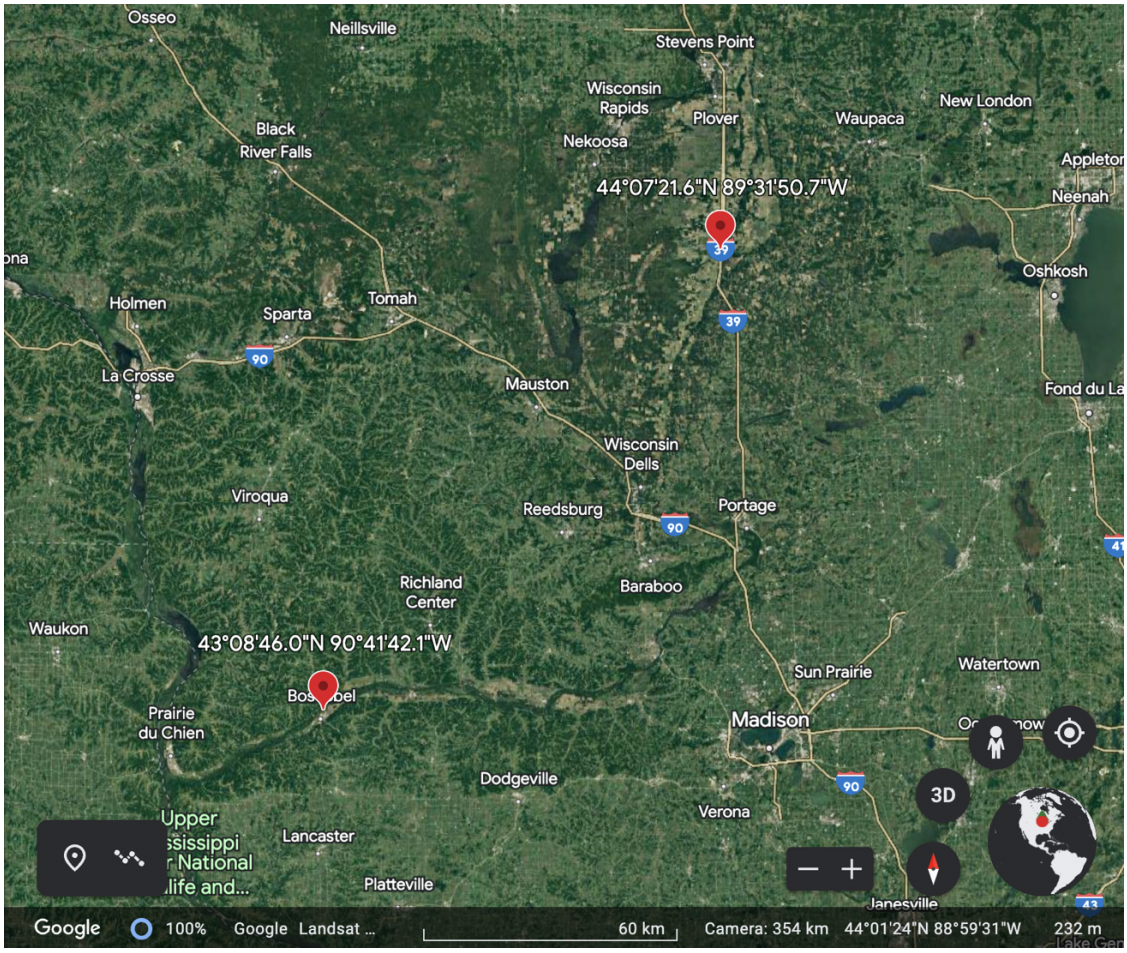

Figure 2.1. The two locations of the two jack pine trees (retrieved from Google Earth)

Production of PyOM

The PyOM was produced from ground jack pine wood (sieved to < 2 mm in diameter) at 350 °C under argon gas (to exclude oxygen) in the charcoalator, which is a modified muffle furnace (Thermo Fisher Scientific 1100 °C Box Furnace BF51800 Series; Güereña et al., 2015). The temperature was ramped to 250 °C in the first 30 minutes, increased to 350 °C over the next 30 minutes, and sustained at 350 °C for another 30 minutes. After that, water was circulated outside the pyrolysis chamber to rapidly cool the PyOM. The PyOM was collected once it reached room temperature. 350 °C is within the temperature range of a typical low-intensity forest fire (Santín et al., 2016). The PyOM yield was 35% of the unburned jack pine wood by dry mass. This PyOM thus represents PyOM produced in the first fire, while the fire simulated in the experimental burns with the calorimeter is considered to be the subsequent fire for the purposes of this experiment.

Determining fire intensity via heat transfer sensing in log burns

In order to ensure the heat treatments are ecologically realistic, we designed experimental log burns to determine the HFs to dose for the High- and Low-HF treatments. The logs used in this experiment were retrieved from the tree we cut in Hancock, WI, which was stored in the drying room at 32 °C and 30% relative humidity for six months. The logs were then oven dried at 105 °C for >48 hours before the burn. A sand bed was prepared and leveled for the burn with three embedded water-cooled HF sensors. Two were Hukseflux combination Gardon and Schmidt-Boelter heat flux sensors with a measurement range of 0-200 kW/m² (model SBG01-200). The third was a Medtherm 64 series Schmidt-Boelter heat flux sensor with a range of 0-114 kW/m² (model 64-10SB-18). The top of the sensors was at the same level as the surface of the sand bed, and they were aligned in the center of the sand bed. One treated log (i.e., with a small groove cut

by hand to increase surface area for combustion) and one untreated log were used for each burn. The treated log was ignited for 10 minutes above four natural gas Bunsen burners (Figure 2.2a) and then placed parallel to the untreated log on the sand bed with the sensors in the middle (Figure 2.2b and 2.2c). The principle for this experiment was to sustain a burn at a relatively small scale and to obtain the HF data between the two logs to input into the calorimeter for burning the PyOM samples.

a)  b)  c) 

Figure 2.2. Log burns setup. a) Treated log on torches; b) the treated (right) and untreated (left) logs on the sand bed for capturing Low HF; c) the treated (right) and untreated (left) logs on the sand bed for capturing High HF

We used the HF data of two 2-log experimental burns to inform two fire scenarios – High HF and Low HF. Both HF profiles were determined from the three sensors between the two logs. For the Low-HF profile, the treated log was of a similar size to the untreated log, and the two logs were not stabilized in place (Figure 2.2b). As the biomass was consumed by fire, the distance between the logs got wider and measured HF declined. For the High-HF profile, we wanted to model higher fuel connectivity and a higher fuel load. Thus, we maintained a relatively constant distance between the two logs and with four steel rods that kept the two logs in place (Figure 2.2c), and used a treated log that was bigger than the untreated log.

The High-HF profile, representing the “high-intensity fire”, was controlled and monitored using LabVIEW (the software that programs the HF profiles, records temperature for each thermocouples, graphs temperature change real time, and controls the HF emitted from the cone

calorimeter, etc.) with a peak HF at 85 kW/m^2 and a duration of 17000 seconds; the Low-HF profile, representing the "low-intensity fire", was modeled with a peak HF at 45 kW/m^2 and a duration of 9000 seconds (Figure 2.3).

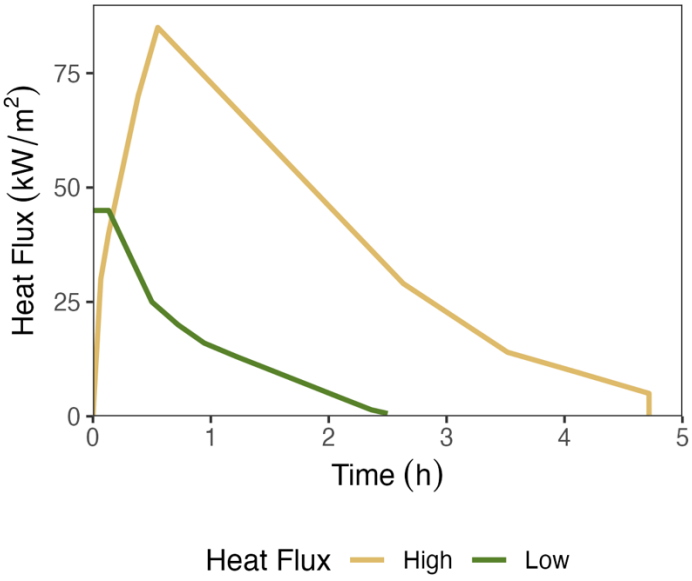

Figure 2.3. High- and low-HF profiles dosed to the samples

Sample treatments and the burning matrix

Three different depths (Surface, 1 cm, and 5 cm) were considered as one variable, and three fire treatments (High HF, Low HF, and Control), were considered as the other variable. They were combined in a full-factorial design, for nine treatments in total, with five replicates each of 1 g PyOM. AquaQuartz Pool Filter Sand (0.45-0.55 mm) was used as the matrix for all the treatments, representing sandy soils typical of jack pine stands while ensuring a C- and nutrient-free system. The sand was treated in advance to further eliminate any traces of C by heating at it 500 °C for three hours in a muffle furnace ("ashed"). Then it was washed with Milli-Q water to flush out any soluble chemicals, oven dried at 100 °C for more than 48 hours, and stored in autoclaved glass bottles.

A burn unit was designed – a steel container filled with the ashed and washed sand. The container was modified from a stainless steel beaker (McMASTER-CARR Stainless Steel Beaker with Handle, 2850 mL capacity, 152.4 mm in diameter and 90 mm in depth). Five PyOM replicates for each fire treatment were placed in the matrix using a custom-designed 3D-printed PLA (polylactic acid filament) sample placer (modeled with Tinkercad; printed with Ultimaker S5, UW Makerspace), which is a flat plate embedded with five identical tubes (Figure 2.4). Each tube has a diameter of 30 mm and a depth of 16 mm. The center of each tube is equidistant (45 mm) to the center of the plate and the same distance (52.9 mm) from the adjacent tubes (Figure 2.4). The sample placer ensured that the samples were placed at the same level in the burn unit and same distance from each other at each treatment.

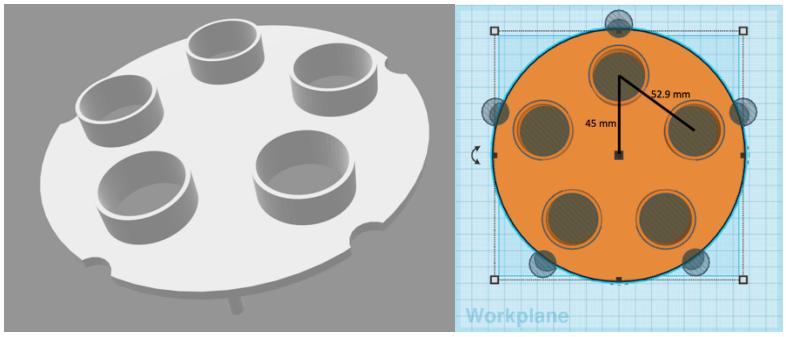

Figure 2.4. Sample placer

To place the samples at different depths for each treatment, we leveled the sand and pressed the sample placer into the sand. Then we scooped out the sand from each tube and filled them with the samples, and gently removed the sample placer. In order to better simulate field conditions, we mixed the 1 g of PyOM with 8 g of sand before burying it. For the 1-cm and 5-cm depths, we added sand to the top of the samples and leveled the top of the matrix at 10 mm from the top of the container. Thermocouples made from 30-gauge type K wire were placed above and below each sample (Figure 2.5a-f).

a)  b)  c)  d)  e)  f) 

Figure 2.5. An example of processes for placing the samples for 1 cm-depth treatments. a) Place the thermocouple wires 16 mm below the designated depth, which is the depth of the sample placer tube; b) Fill the sand to the designated depth and press the sample placer in the sand; c) Scoop out the sand from the tubes, and refill them with the PyOM samples; d) Lift the sample placer with the samples remaining in the sand; e) Place a second set of thermocouple wires on top of the samples; f) Fill the sand in the container to bury the samples (skip this step for surface treatments).

Everything in the burn unit, including the steel container, ring for stabilizing thermocouples, and thermocouples, were weighed individually and all together (with and without putting sand and samples in) before and after the burn to determine total mass loss of the samples and any extra mass loss of the appliances for each treatment. Mass loss fraction and mass remaining (%) were calculated with Equations 2.1 and 2.2:

$$\text{Mass Loss Fraction} = \frac{\text{Mass}_{\text{before}} - \text{Mass}_{\text{after}}}{\text{Mass}_{\text{before}}} \quad (2.1)$$

$$\text{Mass Remaining (\%)} = (1 - \text{Mass Loss Fraction})' 100\% \quad (2.2)$$

Before moving the matrix under the cone calorimeter, an insulation sheet was wired around the container (Figure 2.6) to prevent the thermocouples from being burned and better contain the heat inside the burn unit. The HFs were dosed using the pre-set HF profiles as described above. The temperature data for each thermocouple was recorded by using LabVIEW.

Figure 2.6. Sample matrix with insulation sheet under the cone calorimeter

The cone calorimeter in our experiments was under temperature control mode instead of HF control mode during the burning of the samples. Temperature control mode directly controls the temperature of the cone above the burn unit, while under HF control, it controls the emission of heat based on the HF that the sensor receives, which requires that the sensor be set at the same location as the samples. However, there was not enough space to place the HF sensor and the samples in the same burn unit. Additionally, since the sensor is water-circulated for cooling, it could also cool down the samples if they were placed together. Thus, to ensure that we were able to administer the desired HF during the sample burns, we ran a blank burn for each HF treatment, where only the HF sensors were embedded in the burn unit (no samples), in HF control mode while we also recorded the temperature. Thus, we were able to run the calorimeter in temperature control mode during the experimental burns to achieve the same target HF.

Sample collection

After each burn, the burn unit with the sand matrix was carefully removed from the calorimeter and set in a hood. After the temperature of the samples dropped below 200 °C, we slid a water-circulating ring onto the burn unit to speed up the cooling process and ensure the cooling was even for each replicate (Figure 2.7). After the temperature dropped to 60-80 °C, we took the unit out for sample collection.

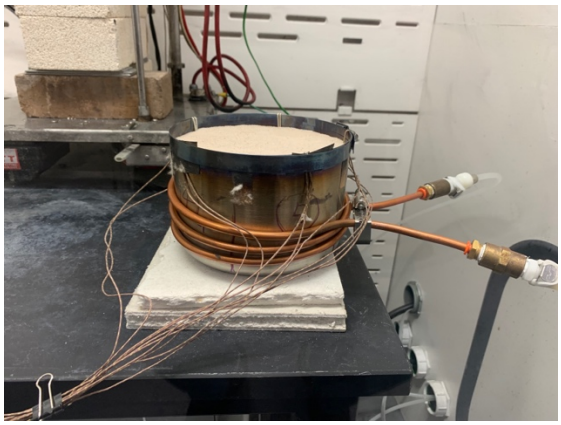

Figure 2.7. Cooling the samples. Burn unit with sand-PyOM matrix is wrapped in water-circulating ring. Thermocouple wires can be seen attached to the burn unit.

In order to ensure we captured as much of the PyOM as possible, we decided to collect and analyze it as a PyOM-sand mixture, rather than trying to physically separate it from the sand matrix. By analyzing blank sand along with sand-PyOM mixtures, we can infer the properties of PyOM without overlooking small particles that are difficult to retrieve, or soluble components that would be lost if we had used a water or other density-based extraction. After cooling, the PyOM samples were scooped out of the sand matrix, along with the surrounding sand to maximize PyOM retrival. For 1 cm and 5 cm samples, before retrieving the samples, the sand on the top was carefully scraped away down to just above the depth where the samples were. After the sample retrieval, we used a custom-designed 3D-printed PLA sample divider (Figure 2.8) (modeled with Tinkercad; printed with Ultimaker S5, UW Makerspace) to collect the rest of the sand (along with any trace amounts of remaining PyOM) in the container. The sample divider includes a cutting end with five wedges that allows it to evenly separate the samples by cutting through the sand, and a container connected to the other end that has five identical chambers to hold the sand in individual sections for each replicate (Figure 2.8). For the unburned controls, PyOM was buried as for the fire treatments, and then retrieved using the same processes as for the burned samples.

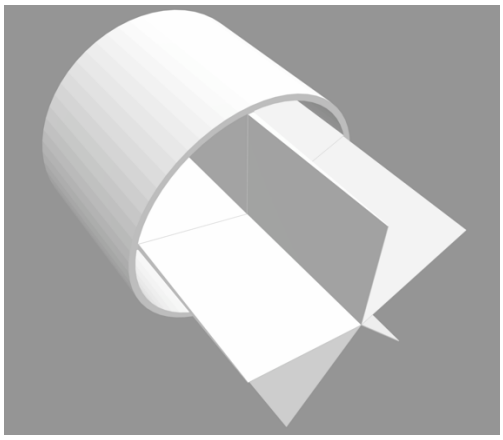

Figure 2.8. Sample divider

The mass of each burned and retrieved PyOM-sand sample was recorded. Before homogenizing the samples, we ensured there was the same mass of sand in each PyOM-sand mixture. We calculated the mean mass loss for all samples in the same treatment, then subtracted it from the original PyOM mass to get the mean remaining PyOM mass in each sample, allowing us to calculate the mass of sand in each mixture. Then we added the sand (from the corresponding section of the matrix where each sample was located) to the sand-PyOM mixture to bring the final mass of the sand to 80 g for each sample. Thus, all final samples had 80 g sand mixed with whatever mass of PyOM out of the initial 1 g remained. For further analysis, all the samples were ground and homogenized individually in FRITSCH Vibrating Cup Mill PULVERISETTE 9 at 1500 rpm for 10 seconds. We also homogenized a subsample of ashed and washed sand, which was used as the sample blank.

Statistical analysis

Calculations and statistical analyses in the table and figures were done using Excel and R (R Core Team, 2022). Figures were created using ggplot 2 (Wickham, 2016) in R (R Core Team, 2022). A 2-way ANOVA with an interaction term for heat flux and burial depth and Tukey's HSD (Tukey, 1949; Graves et al., 2019) were used to determine if there are significant differences

between treatments. A linear model (Oksanen et al., 2022) was used to fit the degree hours and peak temperature as predictors for the fractional mass loss of PyOM.

Results

Qualitative observations

PyOM samples in surface treatments under both HF profiles started to combust in the first 5 minutes. Observations during the experimental burn of the High HF + 1 cm treatment revealed smoke escaping from the burn unit primarily at the beginning of the burn around the first 17 minutes. Those observations implicated that for those three treatments (High HF + Surface, High HF + 1cm, and Low HF + Surface), most chemical reactions and PyOM losses might occur much sooner than the full HF profile's duration, while the mass loss was not able to track during the heating process due to oscillation caused by ambient airflow. Those three treatments also resulted in little visible PyOM left and more than 90% mass loss. No obvious smoke was observed for High HF + 5 cm, low HF +1 cm, and low HF + 5 cm.

Temperature profiles are distinctive across all treatments

Temperature profiles were consistent across replicates and show distinctive patterns for different HF treatments (Figure 2.9). Overall, temperatures decreased with burial depth, and were higher in the High-HF treatments at the same depth. The highest peak temperatures were recorded for surface samples in the High-HF treatment (598.91±23.64°C), while the lowest peak temperature was recorded for 5 cm samples in the low-HF treatment (mean 130.24±0.94°C) (Table 2.1). The peak temperatures reached during the experiment had a time lag from the peak heat flux emitted from the cone calorimeter, following Fourier's Law of heat conduction if viewing the burn unit as a whole object. The temperature profile and peak temperature of the High HF + 5 cm were

similar to those of Low HF + 1 cm treatment (Figure 2.9, blue lines on left and yellow lines on right). Peak temperatures were not significantly different between these two treatments but were significantly different among other treatments ($p < 0.05$, ANOVA in Table S2.1, Tukey's HSD, Table 2.1).

Degree hours (Table 2.1), calculated from the area under the temperature profile, were used to quantify the temperature and duration of heat exposure. The degree hours were significantly different across each treatment ($p < 0.05$, ANOVA in Table S2.2, Tukey's HSD, Table 2.1).

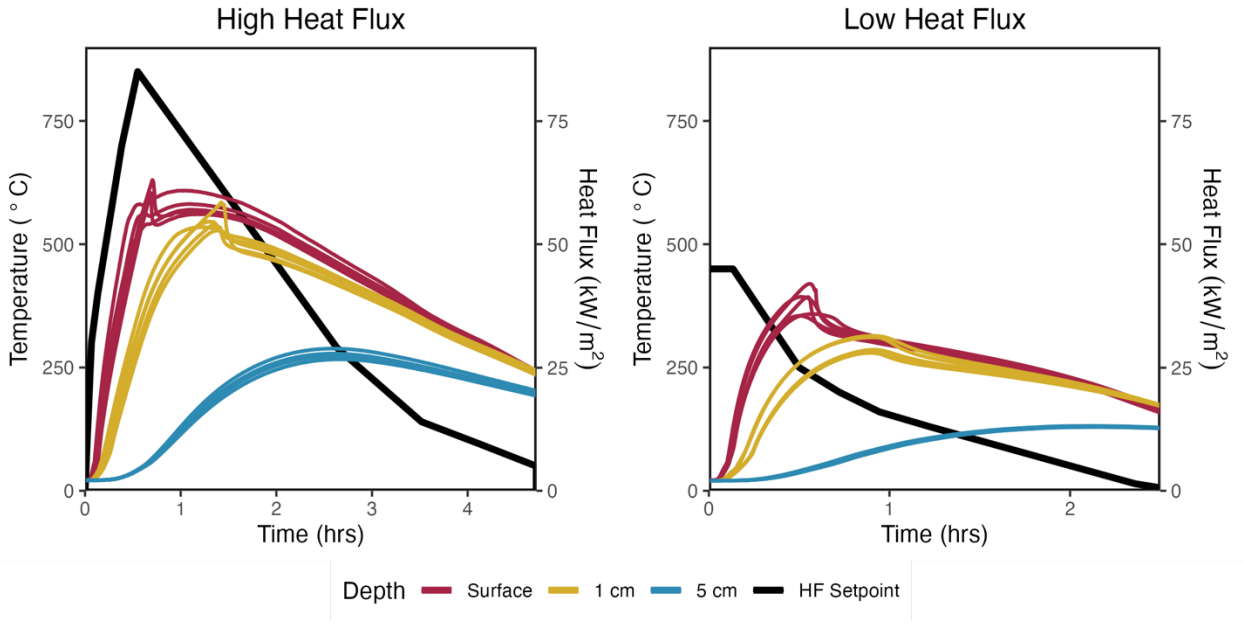

Figure 2.9. Temperature profiles for the bottom thermocouples for five replicate samples in each HF treatment (colored lines) and the corresponding heat flux profiles (black lines), for the High HF (left) and Low HF (right). The temperature data captured by the top thermocouples were not graphed due to excessive oscillations in the near-surface treatment as the thermocouples got exposed to the air (for full temperature profiles, refer to Supplemental Figure S2.1). Note different time scales on x-axis. Samples continued to cool to room temperature beyond data plotted here.

Table 2.1. Degree hours and peak temperature data and statistical results (n=5). Different superscript letters (ANOVA, Tukey's HSD) indicate significant differences across all treatments.

Heat Flux Profiles	**High**	**Low**
Heating Duration (hrs)	**4.72**	**2.5**

Exposure Depth		**Surface**	**1 cm**	**5cm**	**Surface**	**1 cm**	**5 cm**
Degree hours (°C · hrs)	Mean	2006.46[a]	1750.15[b]	928.27[c]	639.10[d]	539.47[e]	224.20[f]
	SD	57.67	49.32	26.98	10.90	24.81	3.04
Peak Temperature (°C)	Mean	598.91[a]	546.39[b]	276.08[d]	383.85[c]	294.64[d]	130.24[e]
	SD	23.64	22.24	8.03	27.16	16.66	0.94

Greater heat exposure leads to higher PyOM mass loss

Mass loss ranged from almost 100% (High HF + Surface and High HF + 1 cm, 98.86% and 98.45%, respectively) to as little as 6.6% (Low HF + 5 cm) (Figure 2.10). Mass loss for High HF + 5 cm, Low HF + Surface, and Low HF + 1 cm were 29.19%, 93.51%, and 47.72%, respectively (Table S2.3). (Note that the entire burn unit was weighed before and after the burn, so we report only the total mass loss of each treatment instead of individual samples.) Peak temperature during the burn was a better predictor for mass loss than degree hours (R^2=0.85 vs. R^2=0.54; Figure 2.11), and greater heat exposure generally led to higher PyOM mass loss.

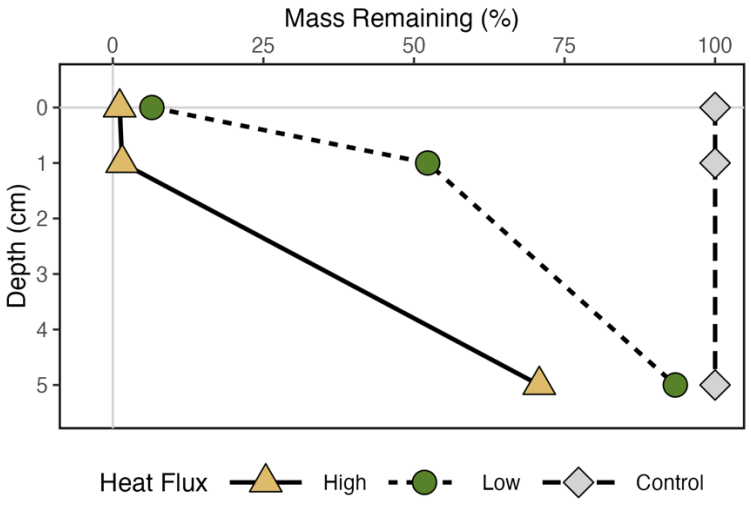

Figure 2.10. Percent of PyOM mass remaining after each treatment

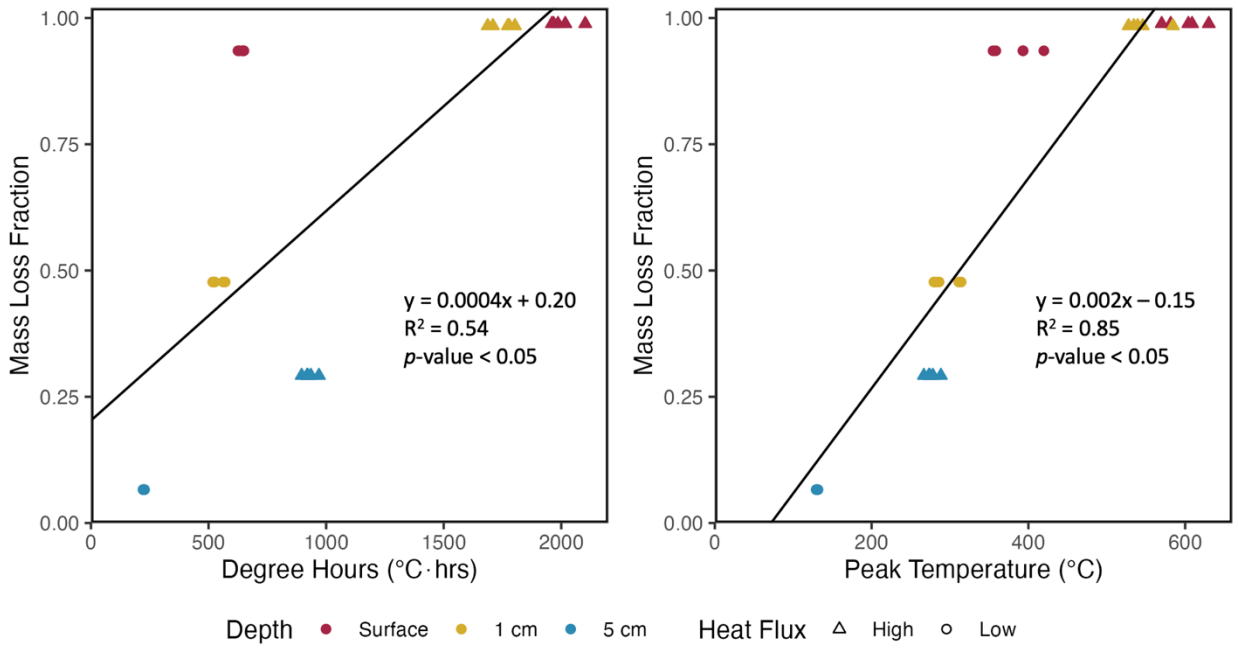

Figure 2.11. Relationship between degree hours (left; line indicates linear model fit; $p < 0.05$ for both slope and intercept; R^2=0.54) or peak temperature (right; line indicates linear model fit; $p < 0.05$ for both slope and intercept; R^2=0.85) and mass loss fraction

Discussion

Highly repeatable laboratory burns

Overall, the processes for fire simulation generate relatively small differences between trials and variations between samples. Although the HF received by the burn unit is not directly monitored by the HF sensors during the experimental burns, we could still ensure the HF-temperature conversion was stable throughout the entire process. After the experimental burns were all completed, the blank burns were conducted again under temperature control mode with only the HF sensor to test if there was any deviation in the HF that the samples received. The results from the last blank burns showed that the heat flux was typically within ±4 kW/m^2 of the prescribed HF profile (refer to Figure S2.2 and S2.3). The High- and Low-HF profiles created distinctive differences in degree hours, peak temperature, and PyOM mass loss. The burn unit setup resulted in very even heat fluxes at a given depth, as indicated by the low standard differences

among thermocouples located at samples within the same treatment. With little variation in the heat profiles dosed to the samples and different effects created by different treatments, this method should be considered promising and repeatable.

Interpretation of the system and potential limitations

Using quartz sand as the media to contain the PyOM samples does not only ensure chemical and physical uniformity, but also simulates the soil texture in typical jack pine barrens. Because quartz has a high melting point (~1700 °C), is chemically inert even during extensive heating, and was ashed and washed before simulations, changes to the PyOM should be the only factor accounting for the difference in chemical properties for different treatments. During a fire under conditions with finer soil textures and different mineralogy, the soil could gain a coarser texture due to the fusion of clay minerals during heating (Badía & Martí, 2003) that would complicate the heat transfer, whereas through our use of quartz, we could ensure a relatively consistent heat transfer due to uniform particle size.

Some moisture would likely be present in the soil of jack pine barrens, even though the soil is sandy and well drained. However, moisture was not incorporated into the experiments for simplification purposes. In general, we would predict that a moist sand matrix would have higher heat capacity due to the presence of water, so it would take more energy for the temperature to increase than the dry sand matrix. Massman (2012) modeled sand heating and moisture transportation and indicated that moisture at and above 35 mm in a sand matrix evaporated at 100 °C within the first hour of heating, and the temperature surged after the water was evaporated. So, it is possible that the near-surface treatments in our experiments are not affected but samples at 5 cm can have more remaining after the burn due to lower temperature at relatively high moisture.

Besides, water can also create anoxic conditions that slow down the oxidation of PyOM during heating.

Although the oxygen (O_2) content in the burn unit was not directly measured, the general burn conditions, particularly for surface treatments, were assumed to be aerobic. For the buried treatments at 1 cm and 5 cm, the aerobic conditions were unknown. In theory, when the surface heating is sufficient to initiate combustion >200 °C, the gas products tend to move upwards and exit the burn unit; and the replenishment of O_2 at deeper soil profiles is much slower than the depletion (Bryant et al., 2005). So, we could assume that the samples in the buried treatments have experienced both aerobic and anaerobic heating. In anaerobic conditions, higher temperatures can lead to more condensed and aromatic structures of PyOM, however, this would not apply to burns with oxygen (Matoszuik et al., 2019), which we expect represents all the treatments of our experiments. The implication of these conditions can be further explored through the analysis of PyOM's chemical and biological properties (Chapter 3).

Buried PyOM can still be combusted in the subsequent fire

The HF profiles we modeled represent different fire intensities. Fire intensity can be related to fire frequency, but the relationship varies across systems and conditions. At least three scenarios could be anticipated: a) systems with higher fire frequencies generally sustain lower-intensity fires due to lower fuel loads; b) however, at the same time, in other systems, short fire return intervals can also result in higher-intensity fires, if the previous fire results in the production of a high fuel load (e.g., snags and down wood); c) in systems with lower fire frequencies, there may be higher accumulation of fuels during the fire return interval, leading to greater heat during burning. The first two scenarios could be applied to our experiment because they are associated with more ground fires while the third scenario is associated with more crown fires. Crown fires usually move

faster and produce PyOM from the woody material, while ground fire can combust PyOM on the forest floor and in the soil (Czimczik & Masiello, 2007). Therefore, fire intensity cannot be the only predictor for PyOM loss or addition during a fire event, while the system in which the fire occurs is also important.

Consistent with our hypotheses, higher HF and shallower depths had more PyOM mass losses. Previous lab and field experiments by Doerr et al. (2018) and Bartoli et al. (2021) determined that low-intensity fires consumed 17-50% of PyOM in mass at the litter surface and soil surface, while high-intensity fires consumed 50-84%. In our study, the mass loss of PyOM at the surface was substantially higher - 93.51% under the Low-HF profile (equivalent to low-intensity fire) and 98.86% under the High-HF profile (equivalent to high-intensity fire). Although less than the mass loss of surface PyOM, our buried PyOM still had substantial mass loss, especially for the PyOM at 1 cm depth under High-HF profile. This likely reflects the fact that our study was designed to represent the upper end of heat fluxes characteristic of realistic surface burns. Therefore, our results would overestimate total PyOM mass loss across a typical burn on a landscape scale but, rather, represent local conditions where logs are burning on the forest floor.

In wildland fires, fire may move quickly on a landscape due to various factors such as wind and topography, so the heating duration may be shorter than the HF profiles; on certain spots where the fuel density is high, it might cause the fire to stay longer. The heating durations for both low-HF and high-HF profiles of our experiments were longer than in most of the existing related studies. However, we found that “degree hours” was a poorer predictor of mass loss than peak temperature (Figure 2.11), indicating that heating duration may not be a key determinant of PyOM mass loss if the heating duration has reached a certain amount of time.

Tinkham et al. (2016) indicated that PyOM is easily degraded by subsequent fires when on the surface or shallow-buried, while thermal degradation is less likely in mineral layers (>30 mm) due to soil insulation. The exposure depths in our study were designed based on this concept. However, substantial thermal degradation still occurred at the depth of 5 cm, particularly under High HF. This can be caused by extensive low-temperature heating. Low-temperature heating (< 300 °C) can also lead to the breakdown of aromatic carbon. Most carbonaceous material can start to be combusted at 150 °C ~ 250 °C (Badía & Martí, 2003; Baldock & Smernik, 2002), however, the exact temperature required for PyOM to be thermally degraded is not well-established. Based on our results, there is even mass loss for PyOM at 5 cm under low HF, which had a peak temperature of less than 150 °C (Table 2.1). For all other treatments, the temperature stayed above 150 °C for an extensive time (Figure 2.9), which can create substantial thermal oxidation. Consequently, we could predict that PyOM even at 5 cm depth in soil profiles can be susceptible to consumption in subsequent fires, as long as the temperature reaches the limits required for thermal degradation.

Conclusion

We presented detailed methods for HF parameterization using log burns and applying the HF profiles to PyOM using a cone calorimeter as the simulation of reburns. We also provided the results of PyOM temperatures during the heating and PyOM mass loss at different exposure depths (surface, 1 cm, and 5 cm) under high- and low-HF profiles. The methods we designed for HF simulation are highly replicable and provide distinctive temperature profiles and heat exposure for each treatment (with shallower depths and higher HFs resulting in higher heat exposure), which could be adopted for further soil heating experiments. We found that deeper burial depths can protect part of PyOM from loss in the subsequent fire, and burial is a more effective protector

under low-intensity fire. Our HF simulations were designed to represent scenarios where there are log burns on the forest floor during a fire event. We would expect HF to be lower on average across the landscape during a given fire, so these results likely represent the upper end of PyOM losses to be expected.

Reference

Ansley, R. J., Boutton, T. W., & Skjemstad, J. O. (2006). Soil organic carbon and black carbon storage and dynamics under different fire regimes in temperate mixed-grass savanna. *Global Biogeochemical Cycles*, *20*(3). doi: 10.1029/2005gb002670

Badía, D., & Martí, C. (2003). Plant Ash and Heat Intensity Effects on Chemicaland Physical Properties of Two Contrasting Soils. *Arid Land Research and Management*, *17*(1), 23–41. doi: 10.1080/15324980301595

Baldock, J. A., & Smernik, R. J. (2002). Chemical composition and bioavailability of thermally altered Pinus resinosa (Red pine) wood. *Organic Geochemistry*, *33*(9), 1093–1109. doi: 10.1016/s0146-6380(02)00062-1

Bartoli, F., Foderi, C., & Mastrolonardo, G. (2021). Effect of repeated burnings, fire and charcoal characteristics on natural charcoal re-combustion in a Mediterranean environment as evaluated in laboratory burning experiments. *Geoderma*, *402*, 115331. doi: 10.1016/j.geoderma.2021.115331

Brodowski, S., Rodionov, A., Haumaier, L., Glaser, B., & Amelung, W. (2005). Revised black carbon assessment using benzene polycarboxylic acids. *Organic Geochemistry*, *36*(9), 1299–1310. doi: 10.1016/j.orggeochem.2005.03.011

Bryant, R., Doerr, S. H., & Helbig, M. (2005). Effect of oxygen deprivation on soil hydrophobicity during heating. *International Journal of Wildland Fire*, *14*(4), 449–455. doi: 10.1071/wf05035

Doerr, S. H., Santín, C., Merino, A., Belcher, C. M., & Baxter, G. (2018). Fire as a Removal Mechanism of Pyrogenic Carbon From the Environment: Effects of Fire and Pyrogenic Carbon Characteristics. *Frontiers in Earth Science*, *6*, 127. doi: 10.3389/feart.2018.00127

Graves, S., Pipepho, H., Dorai-Raj, S. (2019). *multcompView: Visualizations of Paired Comparisons*. https://CRAN.R-project.org/package=multcompView

Gustafsson, Ö., Haghseta, F., Chan, C., MacFarlane, J., & Gschwend, P. M. (1996). Quantification of the Dilute Sedimentary Soot Phase: Implications for PAH Speciation and Bioavailability. *Environmental Science & Technology*, *31*(1), 203–209. doi: 10.1021/es960317s

Hatten, J. A., Zabowski, D., Ogden, A., & Thies, W. (2008). Soil organic matter in a ponderosa pine forest with varying seasons and intervals of prescribed burn. *Forest Ecology and Management*, *255*(7), 2555–2565. doi: 10.1016/j.foreco.2008.01.016

Hobley, E. (2019). Vertical Distribution of Soil Pyrogenic Matter: A Review. *Pedosphere*, *29*(2), 137–149. doi: 10.1016/s1002-0160(19)60795-2

Keeley, J. E. (2009). Fire intensity, fire severity and burn severity: a brief review and suggested usage. *International Journal of Wildland Fire*, *18*(1), 116. doi: 10.1071/wf07049

Massman, W. J. (2012). Modeling soil heating and moisture transport under extreme conditions: Forest fires and slash pile burns. *Water Resources Research*, *48*(10). doi: 10.1029/2011wr011710

Matosziuk, L. M., Alleau, Y., Kerns, B. K., Bailey, J., Johnson, M. G., & Hatten, J. A. (2019). Effects of season and interval of prescribed burns on pyrogenic carbon in ponderosa pine stands in the southern Blue Mountains, Oregon, USA. *Geoderma*, *348*, 1–11. doi: 10.1016/j.geoderma.2019.04.009

Matosziuk, L. M., Gallo, A., Hatten, J., Bladon, K. D., Ruud, D., Bowman, M., … Weiglein, T. (2020). Short-Term Effects of Recent Fire on the Production and Translocation of Pyrogenic Carbon in Great Smoky Mountains National Park. *Frontiers in Forests and Global Change*, *3*, 6. doi: 10.3389/ffgc.2020.00006

Oksanen J., Simpson G., Blanchet F., Kindt R., Legendre P., …, Weedon J. (2022). *vegan: Community Ecology Package*. https://CRAN.R-project.org/package=vegan

Radeloff, V. C., Mladenoff, D. J., He, H. S., & Boyce, M. S. (1999). Forest landscape change in the northwestern Wisconsin Pine Barrens from pre-European settlement to the present. *Canadian Journal of Forest Research*, *29*(11), 1649–1659. doi: 10.1139/x99-089

Radeloff, V. C., Mladenoff, D. J., Guries, R. P., & Boyce, M. S. (2004). Spatial patterns of cone serotiny in Pinus banksiana in relation to fire disturbance. *Forest Ecology and Management*, *189*(1–3), 133–141. doi: 10.1016/j.foreco.2003.07.040

Rudolph, T. D., & Laidly, P. R. (1990). Pinus banksiana Lamb. jack pine. *Silvics of North America*, *1*, 280-293.

R Core Team (2022*). R: language and environment for statistical computing. R Foundation for Statistical Computing, Vienna, Austria. URL https://www.R-project.org/.*

Saiz, G., Goodrick, I., Wurster, C. M., Zimmermann, M., Nelson, P. N., & Bird, M. I. (2014). Charcoal re-combustion efficiency in tropical savannas. *Geoderma*, *219*, 40–45. doi: 10.1016/j.geoderma.2013.12.019

Santín, C., Doerr, S. H., Preston, C., & Bryant, R. (2013). Consumption of residual pyrogenic carbon by wildfire. *International Journal of Wildland Fire*, *22*(8), 1072–1077. doi: 10.1071/wf12190

Santín, C., Doerr, S. H., Kane, E. S., Masiello, C. A., Ohlson, M., Rosa, J. M., … Dittmar, T. (2016). Towards a global assessment of pyrogenic carbon from vegetation fires. *Global Change Biology*, *22*(1), 76–91. doi: 10.1111/gcb.12985

Santín, C., Doerr, S. H., Merino, A., Bryant, R., & Loader, N. J. (2016). Forest floor chemical transformations in a boreal forest fire and their correlations with temperature and heating duration. *Geoderma*, *264*, 71–80. doi: 10.1016/j.geoderma.2015.09.021

Soucémarianadin, L., Reisser, M., Cécillon, L., Barré, P., Nicolas, M., & Abiven, S. (2019). Pyrogenic carbon content and dynamics in top and subsoil of French forests. *Soil Biology and Biochemistry*, *133*, 12–15. doi: 10.1016/j.soilbio.2019.02.013

Tinkham, W. T., Smith, A. M. S., Higuera, P. E., Hatten, J. A., Brewer, N. W., & Doerr, S. H. (2016). Replacing time with space: using laboratory fires to explore the effects of repeated burning on black carbon degradation. *International Journal of Wildland Fire*, *25*(2), 242–248. doi: 10.1071/wf15131

Tukey, J. W. (1949). Comparing Individual Means in the Analysis of Variance. *Biometrics*, *5*(2), 99. doi: 10.2307/3001913

Wickham, H. (2016). *ggplot2: Elegant Graphics for Data Analysis*. Springer-Verlag New York. ISBN 978-3-319-24277-4, https://ggplot2.tidyverse.org.

Wickham H, François R, Henry L, Müller K (2022). *dplyr: A Grammar of Data Manipulation_*. https://CRAN.R-project.org/package=dplyr.

Zimmerman, A. R., & Mitra, S. (2017). Trial by Fire: On the Terminology and Methods Used in Pyrogenic Organic Carbon Research. *Frontiers in Earth Science*, *5*, 95. doi: 10.3389/feart.2017.00095

Supplementary Information (Chapter 2)

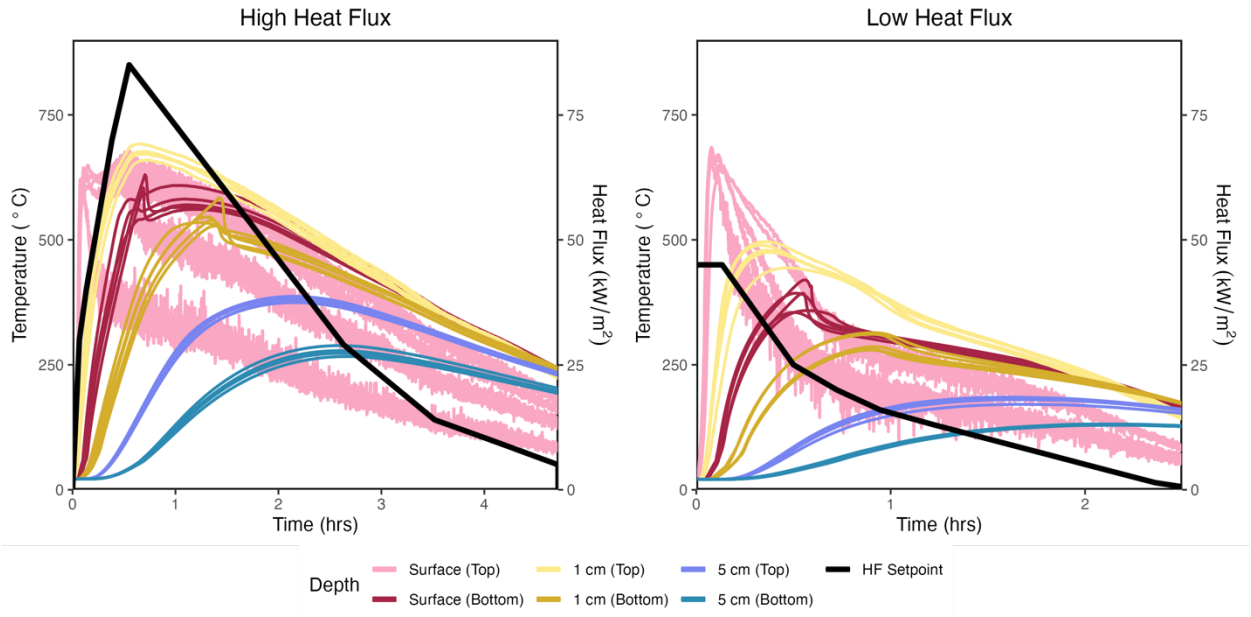

Figure S2.1. Temperature profiles for top and bottom thermocouples for five replicate samples in each HF treatment (colored lines) and the corresponding heat flux profiles (black lines) for High HF (left) and Low HF (right). Note different time scales on x-axis. Samples continued to cool to room temperature beyond data plotted here.

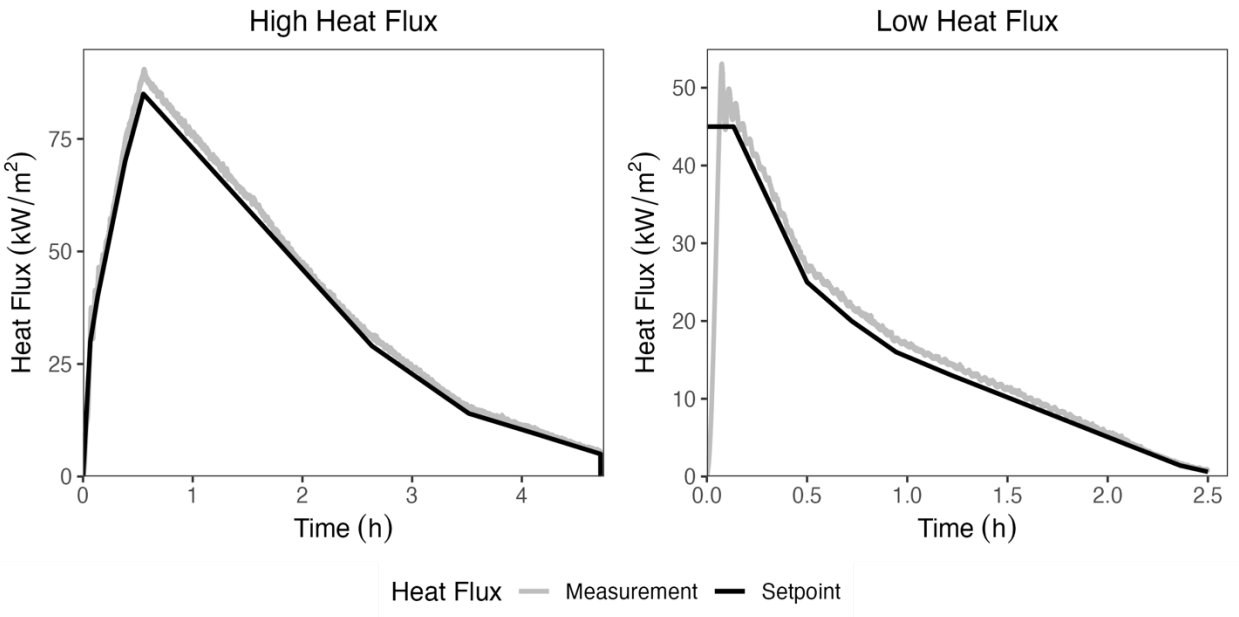

Figure S2.2. Comparison of the heat flux profiles (black line) with the heat flux detected by the sensor during the last blank burn under temperature control mode (grey line) for High HF (left) and Low HF (right). Note different time scales on x-axis.

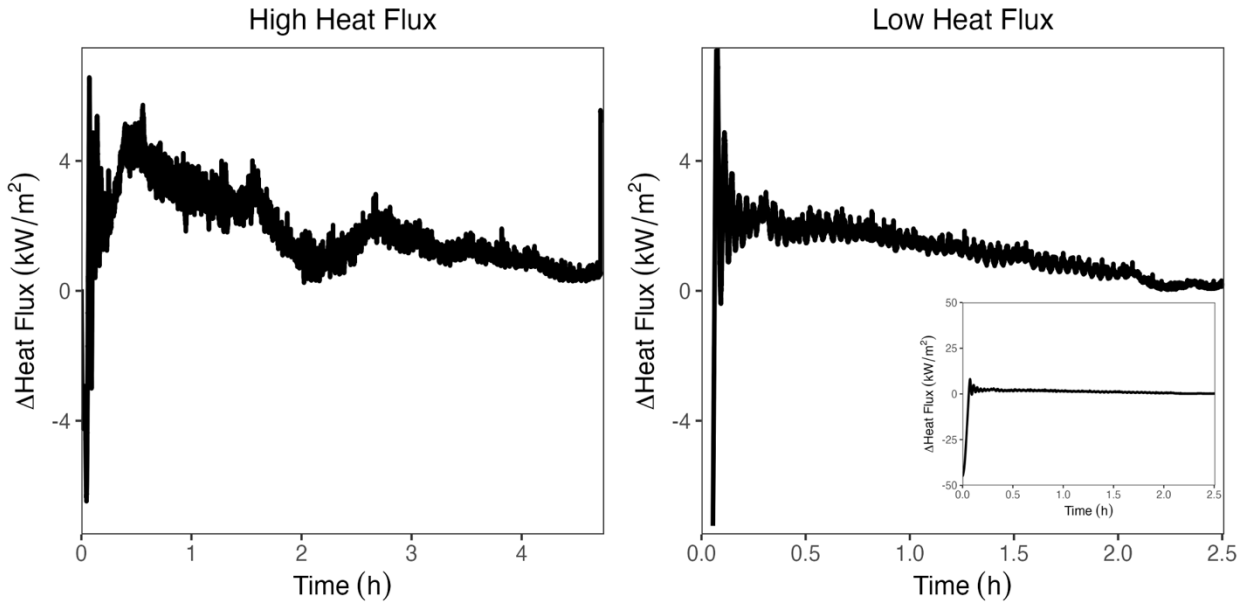

Figure S2.3. Difference between heat flux profiles with the heat flux detected by the sensor during the last blank burn under temperature control mode for High HF (left) and Low HF (right). ΔHeat Flux (kW/m^2) = Measured heat flux – Heat flux setpoint.

Table S2.1. ANOVA statistics for peak temperature (°C)

Sources	df	Sum of Squares	Mean Squares	F statistic	p-value

Heat Flux	1	312785	312785	879.48	$< 2 \cdot 10^{-16}$
Depth	2	451137	225568	634.25	$< 2 \cdot 10^{-16}$
Heat Flux · Depth	2	14462	7231	20.33	$6.83 \cdot 10^{-6}$
Residuals	24	8536	356		

Table S2.2. ANOVA statistics for degree hours (°C · hrs)

Sources	df	Sum of Squares	Mean Squares	F statistic	p-value
Heat Flux	1	8976887	8976887	7449.7	$< 2 \cdot 10^{-16}$
Depth	2	3040982	1520491	1261.8	$< 2 \cdot 10^{-16}$
Heat Flux · Depth	2	600963	300481	249.4	$< 2 \cdot 10^{-16}$
Residuals	24	28920	1205		

Table S2.3. Mass loss fraction for all treatments

Heat Flux	**Depth**	**Mass Loss Fraction (%)**
High	Surface	98.86
High	1cm	98.45
High	5cm	29.19
Low	Surface	93.51
Low	1cm	47.72
Low	5cm	6.60
Control	Surface	0.00
Control	1cm	0.00
Control	5cm	0.00

Chapter 3: Fire Removes Preexisting Pyrogenic Organic Matter from the Ecosystem through the Mechanisms of Both Direct Consumption and Increasing Mineralizability

Introduction

As the second largest pyrogenic carbon (PyC) pool in the world (Bird et al., 2015; Santín et al., 2016), soil PyC has great implications for the carbon (C) cycle. Globally, soil PyC relative to total soil organic carbon (SOC) ranges from less than 1% to up to 45% (Forbes et al., 2006). Regionally, soil PyC stocks vary with many factors, such as land cover, land use, climate, and topography (Abney & Berhe, 2018). PyC is generally described as a form of highly aromatic, condensed (Matosziuk et al., 2019; Preston & Schmidt, 2006), and persistent carbon (C) that has a relatively long residence time (Deluca & Aplet, 2008). When C is described as "persistent", it generally means that the C is resistant to degradation and remains sequestered in the soil matrix, which is a key process for slowing down the global C cycle and mitigating global warming.

PyC is the major component of pyrogenic organic matter (PyOM) and they are effectively the same material, as PyC is the C in PyOM. PyOM has a heterogeneous chemical composition (Bird et al., 2015; Boot et al., 2004). Although relatively resistant to biological decomposition (DeLuca & Aplet, 2008) and tending to have a high persistence in soils, PyOM and PyC are certainly not inert, and the properties and mechanisms governing their dynamics in soil remain under-characterized (Santos et al., 2012; Singh et al., 2012). Soil PyOM and PyC can be decomposed physically, chemically, and biologically; and their persistence is also determined by both chemistry and environment (Knicker, 2011). However, in addition to standard mechanisms of loss, combustion or alteration in subsequent fires may represent an important pathway of PyOM and PyC losses. The first quantitative data on the loss of preexisting PyOM with subsequent fire was in 2013 with mass loss presented (Santín et al., 2013), and it demonstrated that fire is a

consumption mechanism for preexisting PyOM. However, our holistic understanding of the properties of PyOM influenced by fire is still insufficient.

In general, as part of SOC, key processes for PyC in an ecosystem also follow the basic soil forming processes – additions, losses, translocation, and transformation. Given that fire is the major driver of the PyC cycle (Preston & Schmidt, 2006; Santin et al., 2016), each of these processes is also influenced by fire.

Additions

Fire is the major process, and effectively the only process, to create net additions of PyOM in nature. Fire can produce PyC from plant materials, litter, and soil organic matter (SOM), adding to the persistent C pool (Abiven & Santín, 2019; Ohlson et al., 2009).

Losses

Losses of PyOM and PyC usually happen from oxidation, with the final product of CO_2. Loss from subsequent fire (oxidation under heating), is the main pathway for the loss of PyC (Preston & Schmidt, 2006). In addition to losses from fire, photooxidation from ultraviolet (UV) light creates a chain reaction and eventually causes the C loss as CO_2. Abiotic chemical oxidation in nature is usually related to exposure to ozone and usually affects soot or other aerosol forms of PyC (Cheng et al., 2006). In many cases, chemical oxidation is also associated with biological oxidation (such as extracellular enzymes) (Allison & Vitousek, 2004), which acts on the surface of SOM and accompanies microbial decomposition. PyOM loss through biological oxidation also results during decomposition, with PyC being respired as CO_2. Decomposition by microbes with higher carbon use efficiency (CUE) could assimilate C and transform it into the form of necromass (Sokol et al., 2022), which removes the C from PyC pool but comprises the stable C pool.

Transformations

Transformation of PyOM and PyC by fire involves changes in its chemical structure. High-intensity crown fire is thought to increase the chemical recalcitrance of the pre-existing PyC (Doerr et. al., 2018). Low-temperature heating (~<250 °C) has been found to lower the chemical recalcitrance of C by depolymerization and dehydration (Santín et. al., 2016), thus the PyC created by low-intensity fire can be chemically altered to be relatively more biodegradable and also more soluble in water, which facilitates its movement into mineral soil.

Other post-fire processes could also facilitate PyC transformation – post-fire PyC can be altered over longer time scales through physical fragmentation, chemical aging, and biological degradation (Dungait et al., 2012; Preston & Schmidt, 2006).

Translocations

During a fire, the translocation of PyC is usually in the form of aerosols or soot, which comprise a small fraction of the total PyC pool (Bird et al., 2015; Santín et al., 2016). They are usually transported by wind and eventually deposited. Both lateral (e.g., surface run-off and aeolian transportation) and vertical (e.g., leaching and biological incorporation) pathways for post-fire soil PyC movement are still poorly characterized due to a lack of quantitative data (Abney & Berhe, 2018; Bird et al., 2015; Santín et al., 2016;). On the global scale, the ocean is the largest pool and ultimate destination for pyrogenic dissolved organic carbon (DPyC), deposited as aerosols or transported in the aquatic system from erosion (Abiven & Santín, 2019; Ding et al., 2014). Therefore, DPyC comprises the major fraction of the PyC in the aquatic system (Dittmar et al., 2012).

As fire is fundamentally related to biogeochemical processes of PyC, our overarching objective was to investigate how subsequent fire influences the chemical properties of the preexisting PyC and the microbial decomposition of the reburned PyC. This project considers three

main factors related to PyC persistence during and after subsequent fires: protection through burial at different depths, changes in potential for leaching and decomposition as dissolved organic carbon (DOC), and changes in biological degradation. We hypothesized that different HFs and depths would influence pH, total C content, DOC, and the mineralized C of the PyOM in the subsequent fire. We expected that higher HFs and shallower depths would result in higher pH but lower total C, mineralized C, and DOC.

Methods

As described in Chapter 2, we exposed the 350 °C jack pine (*Pinus banksiana* Lamb.) PyOM in a sand matrix situated at surface, 1 cm, and 5 cm to high and low heat fluxes, designed to represent different fire intensity, in a cone calorimeter. We measured a range of parameters, including pH, total C and N, DOC, and incubation with KOH traps, to test how different heat exposures affect the chemical and biological properties of PyOM.

pH

For each sample (PyOM-sand mixture) and the sample blank (ground quartz sand), 0.5 g was weighed in a 15 mL Falcon tube and saturated with 0.5 mL of DI water. The samples were saturated for 48 hours before the test. Because the samples were dry from the production through the simulated burns, the initial addition of water likely initiated various chemical reactions within the sample that led to unstable pH values immediately after wetting-up. To allow the sample to settle at a stable pH, we let them sit for 48 hours before measuring pH. This water saturation could also represent the first rain after a fire. After the saturation was completed, another 9.5 mL of water was added to each tube, bringing the solid (g) to liquid (mL) ratio to 1: 20, following Zeba et al. (2022). Then all tubes were oscillated with an INCU-SHAKER 10L (Benchmark Scientific,

Sayreville, NJ, USA) for 10 minutes at 200 rpm and centrifuged with a Centrifuge 5810 R (15 amp version, Eppendorf, Hamburg, Germany) at 3214 rcf (or 3900 rpm, which is the highest limit for the machine) for 15 min. Two replicates of 1 mL of the supernatant solution were extracted from the tube for each sample and measured with a pH electrode InLab Micro (Mettler Toledo, Columbus, OH, USA) connected to a Thermo Scientific Orion Star A215 pH/Conductivity Meter (Thermo Fisher Scientific, Waltham, MA, USA).

Total C

Samples used for measuring total C were dried at 60 °C for 48 hours before preparation. Samples were wrapped in CE Elantech 5 x 9 mm tin capsules (~60 mg, for treatments High HF + 5 cm, Low HF + 1 cm, Low HF + 5 cm, and controls) and 10 x 12 mm tin capsules (200 ~ 400 mg, for treatments High HF + Surface, high HF + 1 cm, and low HF + Surface, which had lower C concentrations) and analyzed using the Thermo Flash EA 1112 NC Analyzer (Thermo Fisher Scientific, Waltham, MA, USA) at the Jackson Lab, UW-Madison. Two replicates were used for each sample and the mean value is presented. C Loss Fraction was estimated using Equation 3.1.

$$\text{C Loss Fraction} = \frac{C_U - C_B}{C_U} \tag{3.1}$$

C_B is the C concentration for the individual sample that has been burned, while C_U is the average value of C concentration for the unburned samples at the same corresponding depth.

12-week incubation with potassium hydroxide (KOH) trap

We incubated samples for 12 weeks with a microbial inoculum to investigate PyC mineralization after subsequent fire. The setup for the 12-week incubation was comprised of a vial of 15 g sample with microbial inoculant added and a vial of 15 mL 0.05 M KOH solution (the CO_2

trap) placed inside a sealed 8 oz (236.6 mL) glass jar (Burch Bottle & Packaging) (Schindelbeck et al., 2016). All samples, along with 3 sample blanks (ground quartz sand) were included in the incubation.

We inoculated each sample with a microbially active soil extraction along with a nutrient solution, which represents the optimal environment for microbial survival. The inoculant for the sample incubation was composed of a microbial extraction from a previously burned soil, collected in 2020, six years after the 2014 King Fire (38.86953, -120.61322) in California (Zeba et al., 2023). The soil is a sandy clay loam, with a pH of 5.7. After the soil was retrieved from the -23 °C freezer and thawed at 4 °C, 5 g of the soil was incubated at 25 °C in a VWR Incubator (Radnor, PA, USA) at 60% water holding capacity (WHC) for 8 days in order to reactivate the microbial community. WHC was determined by saturating the soil on a filter paper in a funnel and draining for 2 hours, then calculating the difference in mass between the saturated soil and the oven-dried soil (Whitman et al., 2013). A similar process was used to determine the WHC for the PyOM-sand samples.

After the incubation, 4.5 g incubated soil was added to 225 mL of DI water (1:50 w/v) and shaken at 100 rpm for 30 minutes. Then the solution was sedimented for 10 minutes and filtered through Whatman 1 filter paper. This extract was mixed with a nutrient solution in a 500 mL volumetric flask (with DI water added to 500 mL). The resulting 500 mL inoculant solution contained the microbial extract, 4 mM NH_4NO_3, 4 mM $CaCl_2$, 2 mM KH_2PO_4, 1 mM K_2SO_4, 1 mM $MgSO_4$, 25 µM H_3BO_3, 2 µM $MnSO_4$, 2 µM $ZnSO_4$, 2 µM $FeCl_2$, 0.5 µM $CuSO_4$, and 0.5 µM Na_2MoO_4 (Cheng et al., 2006; Whitman et al., 2013). 2.05 mL of nutrient solution, representing 55% WHC, was added to each sample. 5 mL of CO_2-depleted DI water was added to the bottom of the jar while placing the sample and KOH vials to maintain the moisture of the system (Whitman et al., 2014).

For each sample, the vial of KOH solution was retrieved and replaced with a new vial of KOH solution 2 weeks, 4 weeks, 8 weeks, and 12 weeks after the start of the incubation. At each retrieval, the electric conductivity (EC) of the KOH vial was measured with an Orion DuraProbe Conductivity Probe connected to the Orion Star A215 pH/Conductivity Meter (Thermo Fisher Scientific, Waltham, MA, USA). The EC of the new KOH solution was also recorded at the beginning of the incubation and during each retrieval.

The KOH trap is used because KOH reacts with CO_2 to produce K_2CO_3 (Equation 3.2), which causes a linear change in EC. Based on the change of EC, we can calculate how much CO_2 is emitted (Equation 3.3).

$$2\mathrm{KOH} + \mathrm{CO_2} \rightarrow \mathrm{K_2CO_3} + \mathrm{H_2O} \tag{3.2}$$

We also ran a "blank incubation" to test how much CO_2 is emitted from the dissolution of inorganic C (especially for the treatments with higher ash production). This set of incubation trials was inoculated with only nutrient solution (substituting the microbial extract with DI water), filtered through a 0.2 μm cellulose acetate sterile syringe filter to minimize the potential for contamination by microbes.

Mineralized C and mineralizability

The calculation of C loss as CO_2 (CO_2-C, in grams) follows Equation 3.3 (Johnson et al., 2023; Schindelbeck et al., 2016; Strotmann et al., 2004).

$$\mathrm{CO_2 - C} = \frac{EC_{raw} - EC_{fin}}{EC_{raw} - EC_{sat}} \cdot V \cdot C_{KOH} \cdot A \cdot M_{CO_2} \cdot \frac{M_C}{M_{CO_2}} \tag{3.3}$$

EC_{raw} is the EC measured for pure 0.05 M KOH. EC_{sat} is the EC measured for 0.025 M K_2CO_3 (the result when all OH ions have reacted with CO_2). EC_{fin} is the EC measured at each

retrieval. V is the volume of the KOH trap in liters (0.015 L). C_{KOH} is the molarity of the KOH trap (0.05 M). A is the ratio of CO_2 needed to react with one portion of KOH (0.5). M_{CO_2} is the molar mass of CO_2 (44.01 g·mol^{-1}) and M_C is the molar mass of C (12.011 g·mol^{-1}). Measurements from the sample blanks were averaged and deducted from each sample to account for CO_2 present in the jars when they were sealed.

In order to reflect the relative mineralizability of the samples, we also reported the fraction of total C (g CO_2-C per g total C) respired as CO_2 during the entire 12-week incubation (C_{min}, Equation 3.4). C_B is the C concentration for each sample (Equation 3.1), and m is the sample mass used for incubation (15 g).

$$\mathrm{C_{min}} = \frac{\mathrm{CO_2 - C}}{\mathrm{C_B} \cdot m} \tag{3.4}$$

Fraction of C remaining (C_r) after mineralization was calculated with Equation 3.5.

$$\mathrm{C_r} = 1 - \mathrm{C_{min}} \tag{3.5}$$

Dissolved organic carbon

DOC samples were prepared with a 1:3 water:volume ratio for the sample and DI water (7 g sample with 21 mL DI water). Samples were oscillated at 150 rpm for 60 minutes and centrifuged at 2000 rcf for 10 minutes (Hofmann et al., 2012; Jones & Willett, 2006). The supernatant of the solution was extracted by a syringe and filtered through the GD/X 25 mm Sterile Syringe Filter (glass microfiber filtration medium, 0.45 µm) into 17 mL TOC tubes (ashed at 450°C for 8 hours in the muffle furnace). All the samples were prepared with the extraction process within 24 hours of analysis and stored at 4 °C before testing with the analyzer. DOC was measured using a Sievers M5310 C Laboratory TOC Analyzer System with GE Autosampler (General Electric, Boston, MA, USA) at the Water Science and Engineering Laboratory, UW-Madison. While the raw DOC data

are reported as ppm, or $mg \cdot L^{-1}$, to better present the data, Equation 3.6 was used to change the unit to "mg DOC per g of PyOM-sand sample".

$$\mathrm{DOC} = C_{DOC} \cdot \frac{V}{m} \tag{3.6}$$

C_{DOC} is the concentration of DOC in $mg \cdot L^{-1}$. m is the mass of sample (7g) for DOC extraction. V is the volume of DI water (in liters) added to sample (0.021 L). Dissolved inorganic carbon (DIC) was also calculated with the same equation.

Statistical analyses

Calculations were performed in Excel and R (R Core Team, 2022). A 2-way ANOVA with an interaction term for heat flux and burial depth and Tukey's HSD (Tukey, 1949; Graves et al., 2019) were used to determine if there were significant differences between treatments for pH, total C, mineralized C, DOC, and DIC. A one-way ANOVA and Tukey's HSD (Tukey, 1949; Graves et al., 2019) were used to determine if there were significant differences between treatments (all combinations of HF and Depth) for C mineralizability, degradable C fraction, and C degradation speed (data from High HF + Surface and High HF + 1 cm was excluded due to unquantifiable total C). Linear models (Oksanen et al., 2022) were used to fit 1) the mass loss fraction of PyOM as the predictor for the C loss fraction, 2) degradable C fraction as predictor for C mineralizability, 3) DOC and DIC as predictors for pH, and 4) DOC as predictor for mineralized C.

A quadratic model (Elzhov et al., 2023) was used to fit the peak temperature of PyOM as the predictor for pH (Equation 3.7). The purpose for this model is to find out what temperature could lead to the lowest pH of PyOM. y represents predicted pH, x represents corresponding peak temperature, $-\frac{b}{2a}$ represents the temperature corresponding to the lowest pH.

$$y = ax^2 + bx + c \quad (3.7)$$

A one-pool decay model (modified from Singh et al., 2012) (Equation 3.8) was used to fit the values of C_r (Equation 3.5) for each treatment (Elzhov et al., 2023). It was used to model the C degradation based on the C mineralization data.

$$C_M = a \cdot e^{-b \cdot t} + (1 - a) \quad (3.8)$$

C_M is the modeled fraction of C remaining. a is the readily degradable fraction of C, and b is the degradation rate (per week). t is the time (in weeks) after the start of incubation. The first part of the equation represents a typical decay model – because the PyC is so persistent, a simple exponential decay model did not fit the data well, so we added the second term (1-a) to allow a to represent the non-decomposable fraction of C.

All the figures for visualizing data were made using ggplot2 in R (Wickham, 2016).

Results

As heat exposure increased, pH decreased at first, then increased

Both HF and burial depth significantly changed the pH of PyOM ($p < 0.05$, ANOVA in Table S3.1, Tukey's HSD, Figure 3.1a), with initial decreases as peak temperature increased, switching to increases as peak temperature reached its highest values. We found that the pH of the samples significantly increased on the surface and at 1 cm with high HF, and decreased at the intermediate heat exposure (High HF + 5 cm and Low HF + 1 cm). For Low HF + Surface and Low HF + 5 cm, the pH of PyOM was not significantly different from the controls. Based on the quadratic model fit, we found that when peak temperature increased to 200 °C, pH hit the lowest value (Figure 3.1b). Therefore, we might predict the lowest pH values to occur around peak

temperature 200 °C, while the lowest measured pH occurred around peak temperatures of 266 ~ 314 °C.

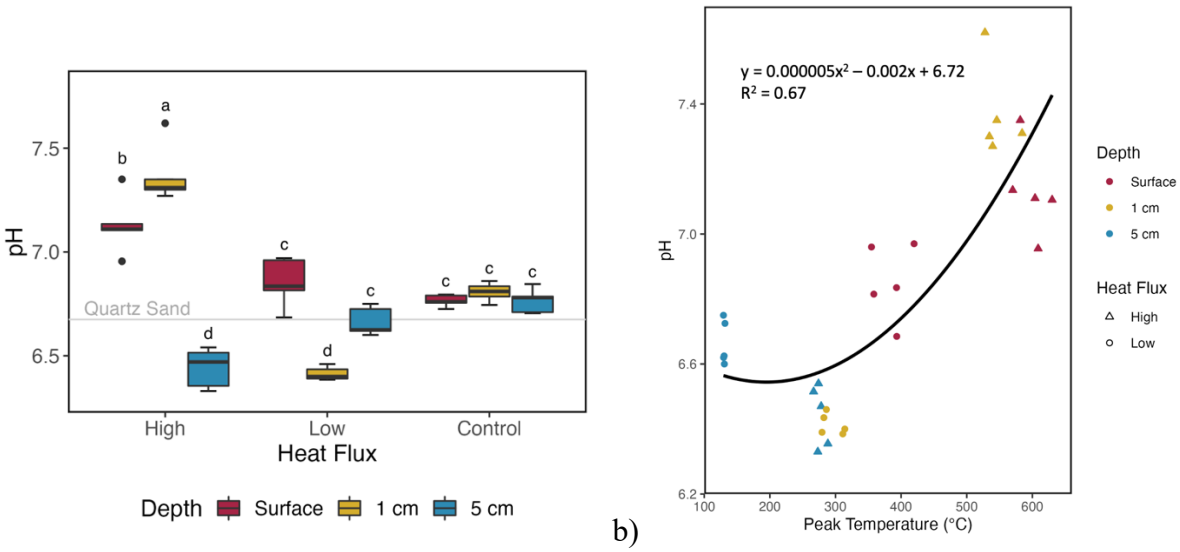

Figure 3.1. a) pH of each treatment (n = 5, $p < 0.05$; grey line indicates pH value of sample blank; letters indicate significant differences; ANOVA, Tukey's HSD); b) pH vs. the peak temperature of PyOM (curve indicates quadratic fit; p for coefficient a and c < 0.05, p for coefficient b > 0.05; $R^2 = 0.67$)

Carbon loss followed trends of mass loss

The C concentration in all samples were below or around 1% (Figure 3.2a) from the dilution by sand. The C concentration of High HF + Surface and High HF + 1 cm treatments were below the quantification limit, which is < 0.05% (Figure 3.2a), indicating near-complete combustion. Most samples also had N contents below the quantification limit except for a few controls (which were < 0.03%), so the data for N concentrations are not presented. In general, both HF and burial depth significantly influenced the C loss of PyOM ($p < 0.05$, ANOVA in Table S3.2, Tukey's HSD, Figure 3.2a). At the same exposure depth, High HF caused more C loss than Low HF; while under the same HF, C loss decreased as burial depth increased (Figure 3.2a). The linear model fit indicates that the mass loss fraction of PyOM closely mirrors the fractional C loss (Figure 3.2b, R^2=0.98).

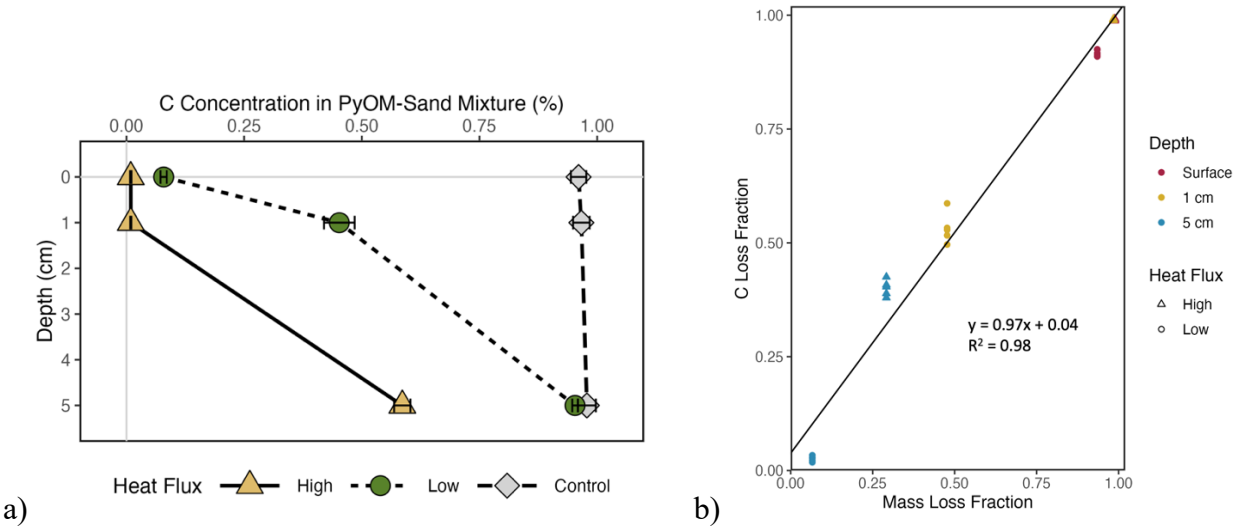

a) b)

Figure 3.2. a) C concentration for samples in each treatment (n = 5, $p < 0.05$; ANOVA); b) C loss fraction vs. PyOM mass loss fraction (line indicates linear model fit; $p < 0.05$ for both slope and intercept; R^2=0.98)

Intermediate-to-high heat exposure increased PyOM susceptibility to loss via microbial decomposition after fire

Over the 12-week incubation, we found more C was mineralized in the treatments High HF + 5 cm and Low HF + 1 cm compared to Low HF + 5 cm and the controls; while less C was mineralized in the treatments High HF + Surface, High HF + 1 cm, and Low HF + Surface, which correspond to higher heat exposure ($p < 0.05$, ANOVA in Table S3.3, Tukey's HSD, Figure 3.3a). For Figure 3.3a, one outlier from the treatment High HF + Surface was removed for extremely high respiration (possibly due to a leak in the jar or sample contamination). We also found higher mineralizability in treatments High HF + 5 cm, Low HF + Surface, and Low HF + 1 cm, comparing to Low HF + 5 cm and the controls ($p < 0.05$, ANOVA in Table S3.4, Tukey's HSD, Figure 3.3b). So, in general, intermediate heat exposure led to more mineralized C and higher C mineralizability, and higher heat exposure could also lead to higher C mineralizability (not mineralized C due to limited amount of residual PyC).

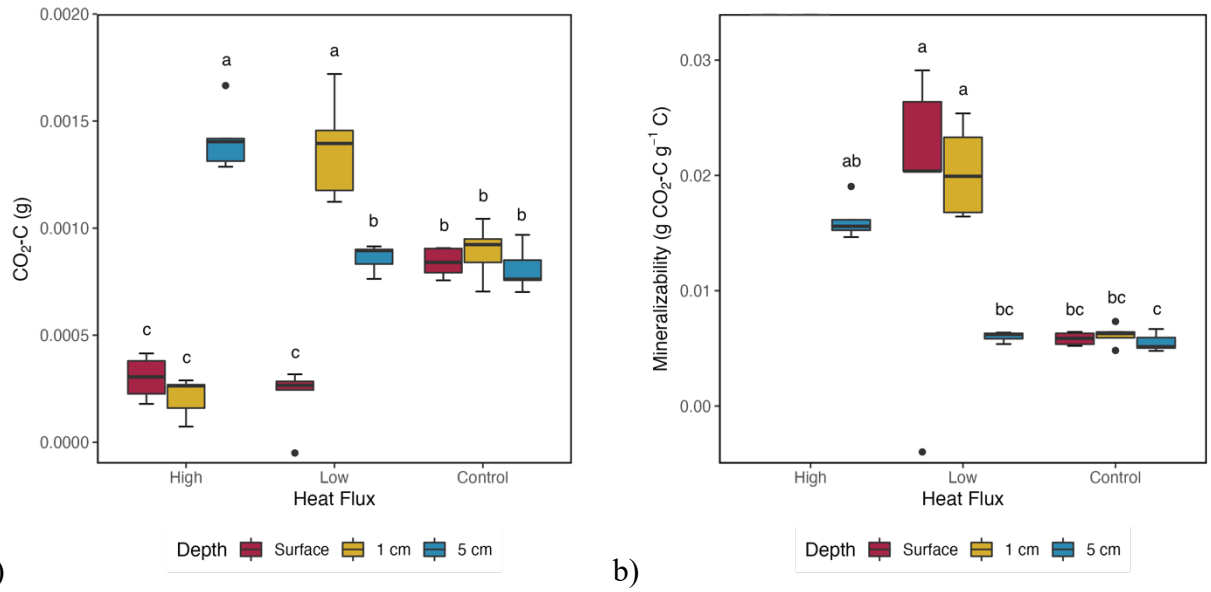

a) b)

Figure 3.3. a) C loss as CO_2 from microbial mineralization (n = 5; $p < 0.05$; one outlier removed from High HF +Surface; letters indicate significant differences (ANOVA, Tukey's HSD)); b) Mineralizability for PyOM in each treatment (n = 5; $p < 0.05$; excluded High HF + Surface and High HF + 1 cm due to unquantifiable total C; letters indicate significant differences (ANOVA, Tukey's HSD))

We fitted the one-pool decay model with the remaining C during the 12-week incubation over time and found good fits for most of the samples (Figure 3.4). For the model-fitting, we excluded the treatments High HF + Surface and High HF + 1 cm due to the total C concentration below the quantification limit. Based on Figure 3.4, CO_2 production rate generally declined over time, and most respiration occurred in the first few weeks. One sample in the Low HF+ Surface treatment was not fit with the decay model due to a presumably erroneous negative C mineralization measured C on Week 12 (Figure 3.4, top middle panel), so we excluded this sample as an outlier in the further ANOVA analyses.

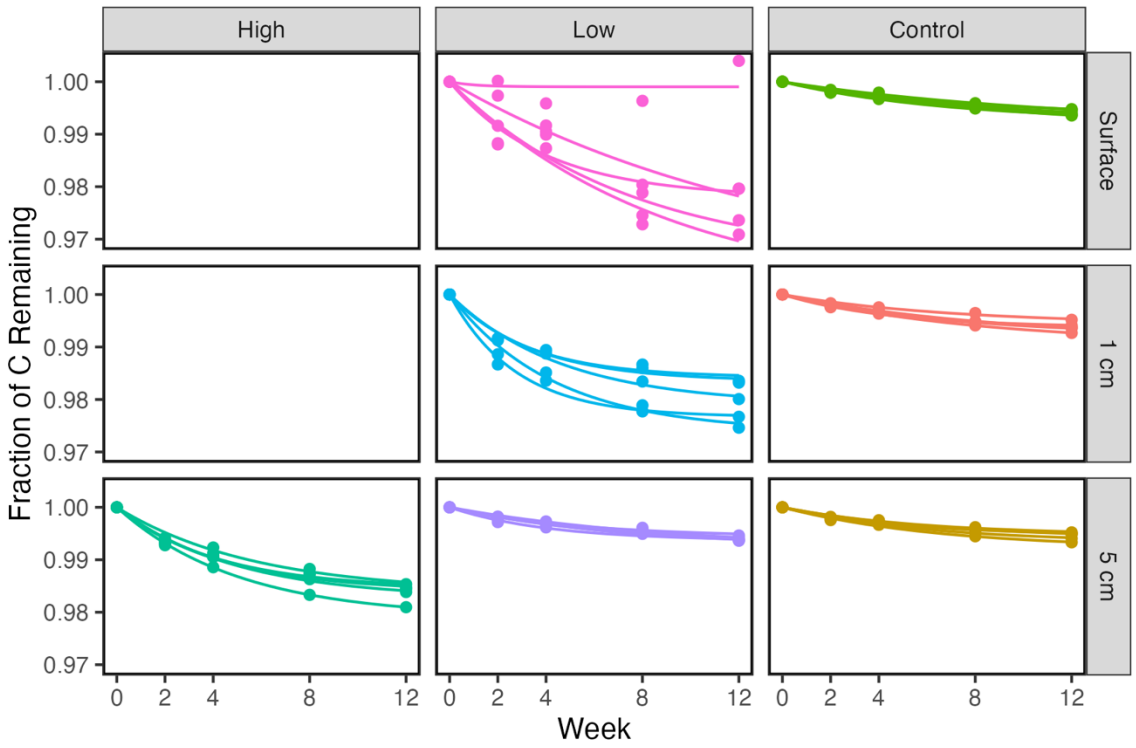

Figure 3.4. One-pool decay model fitting with the remaining C after microbial degradation over 12 weeks (n = 5; excluded High HF + Surface and High HF + 1 cm for unquantifiable total C; one outlier in Low HF + Surface still presented in the graph but excluded in further analysis)

For coefficients a and b (Equation 3.8) in the decay model, which indicate degradable C fraction and degradation speed respectively, we treated them as observations and performed one-way ANOVA analysis to test for significant differences between treatments. We found treatments High HF + 5 cm, Low HF + Surface, and Low HF + 1 cm had higher degradable C fraction than Low HF + 5 cm and the controls ($p < 0.05$, ANOVA in Table S3.5, Tukey's HSD, Figure 3.5a), while Low HF + 1 cm had higher degradation rates than all other treatments except for High HF + 5 cm ($p < 0.05$, ANOVA in Table S3.6, Tukey's HSD, Figure 3.5b).

In general, based on the coefficients of the one-pool decay model (Figure 3.5 a & b), mineralized C, and mineralizability (Figure 3.3 a & b), the biological properties for PyOM treated with Low HF + 5 cm were not significant different from the controls. Biological properties for PyOM with other treatments were all different from the controls. We also found a linear correlation

between the degradable C fraction and mineralizability (Figure 3.6), which further testified to the fitness of the decay model.

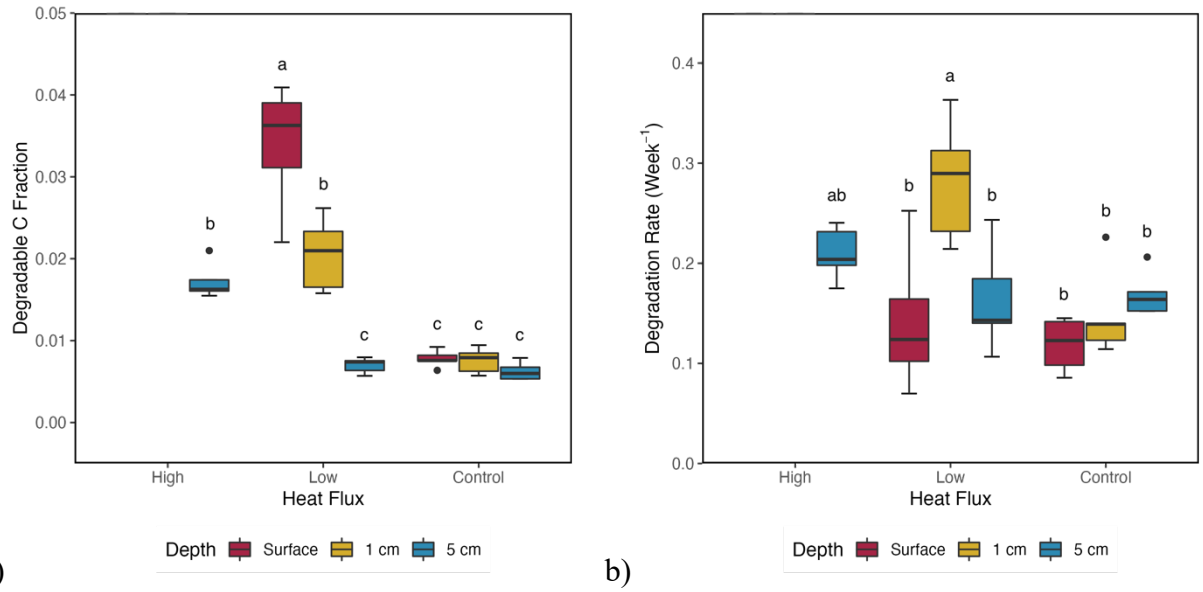

a) b)

Figure 3.5. a) Degradable C fraction (*a*) of the samples from the decay model (n = 5; $p < 0.05$; excluded one outlier in Low HF + Surface); b) Degradation rate (*b*) of the samples from the decay model (n = 5; $p < 0.05$; excluded one outlier in Low HF + Surface)

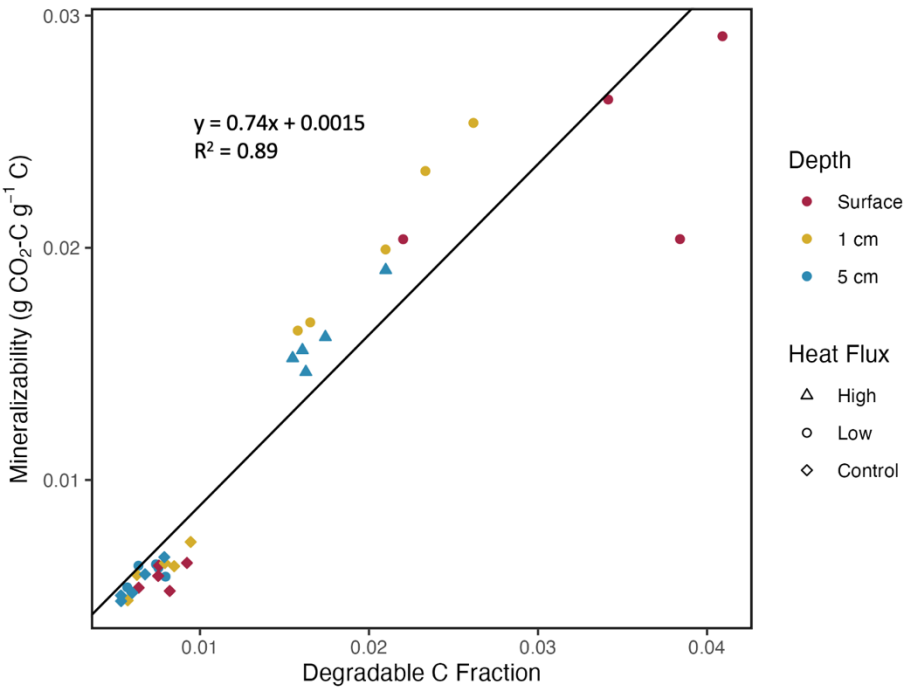

Figure 3.6. Mineralizability vs. Degradable C Fraction (line indicates linear fit; $p < 0.05$ for slope and intercept; $R^2 = 0.89$)

More DOC is produced from preexisting PyOM at intermediate heat exposure

After the subsequent burns, DOC significantly increased in treatments with intermediate heat exposure (High HF + 5 cm and Low HF + 1 cm) ($p < 0.05$, ANOVA in Table S3.7, Tukey's HSD, Figure 3.7a) and DIC significantly decreased in treatment High HF + 5 cm ($p < 0.05$, ANOVA in Table S3.8, Tukey's HSD, Figure 3.7b). We could potentially conclude that treatments with lower peak temperatures tended to increase DOC and decrease DIC, whereas the highest peak temperature tended to lose DOC and increase DIC.

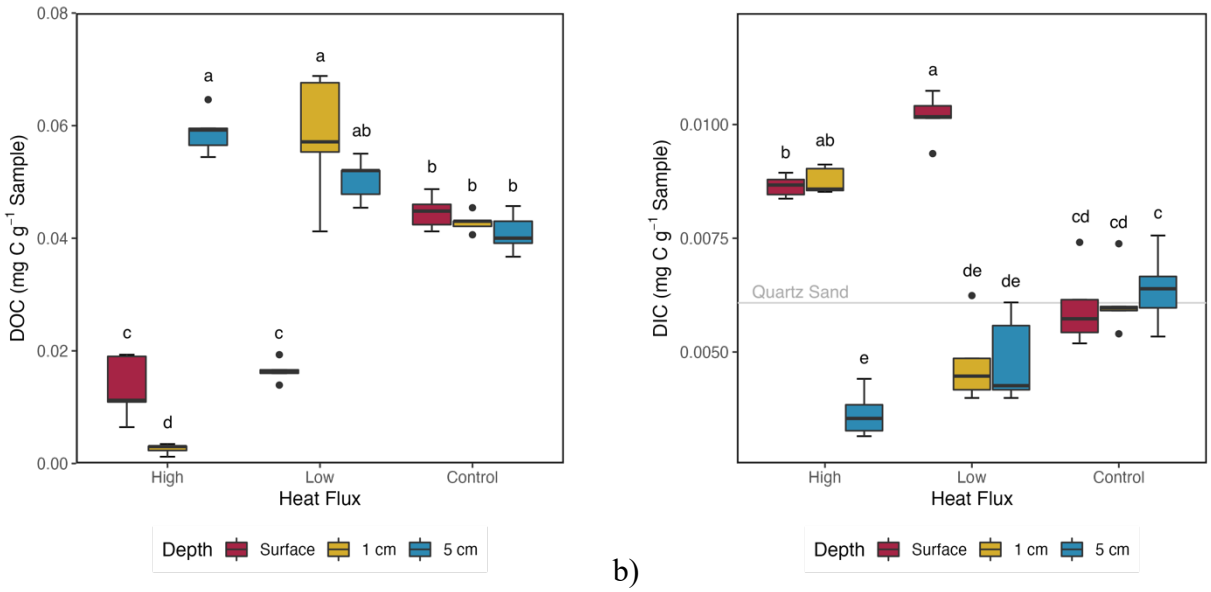

a) b)

Figure 3.7. a) DOC of samples. Letters indicate significant differences (ANOVA, Tukey's HSD, $p < 0.05$); b) DIC of samples. Letters indicate significant differences (ANOVA, Tukey's HSD, $p<0.05$). Grey line indicates sample blank.

Based on the linear fitting of pH vs. DOC and pH vs. DIC, we found that pH generally deceased with the DOC concentration (R^2=0.78; Figure 3.8a) while it increased with DIC concentration (R^2=0.54; Figure 3.8b). DOC was also positively correlated with mineralized C after 12 weeks (R^2=0.83, Figure 3.9)

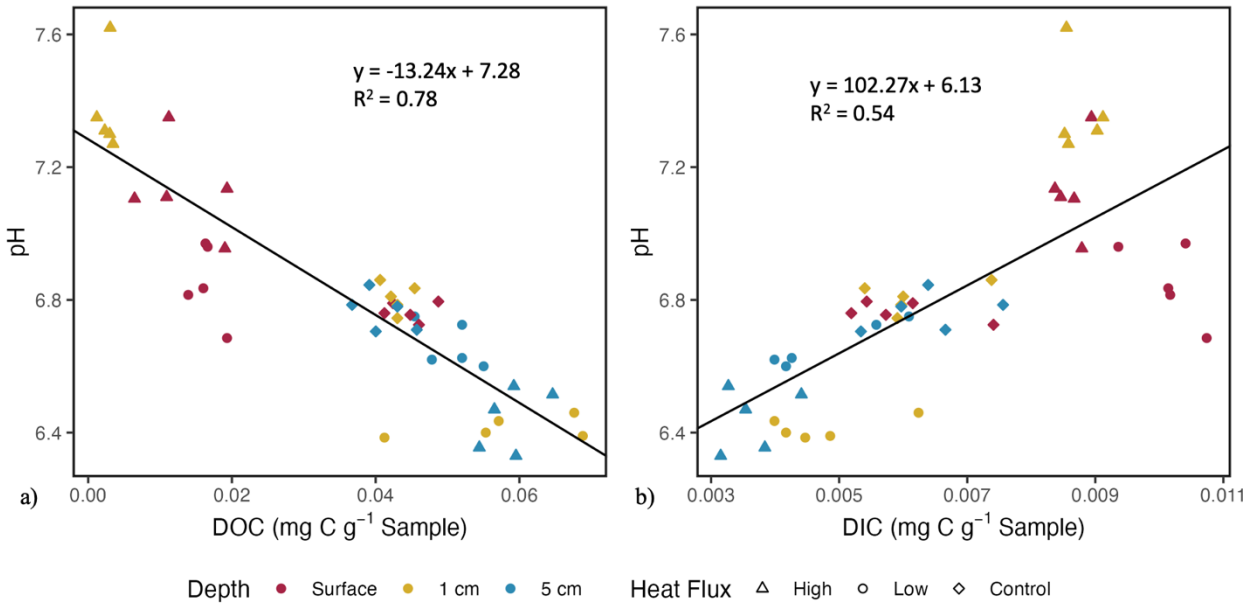

Figure 3.8. a) pH vs. DOC (line indicates linear fit; $p < 0.05$ for both slope and intercept; $R^2 = 0.78$) b) pH vs. DIC (line indicates linear fit; $p < 0.05$ for both slope and intercept; $R^2 = 0.54$).

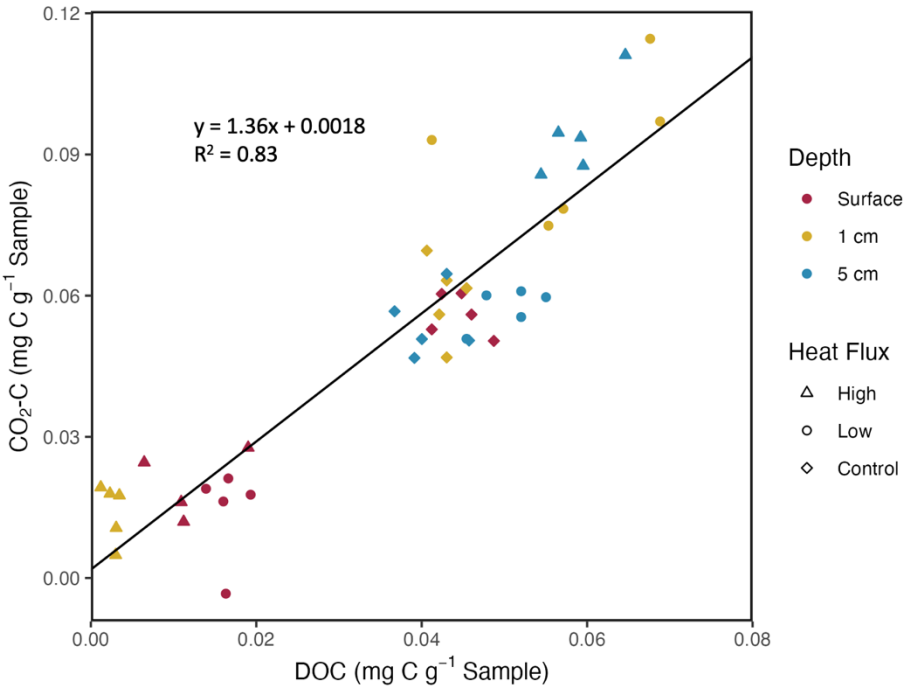

Figure 3.9. CO_2-C vs. DOC (line indicates linear fit; $p < 0.05$ for slope; $R^2 = 0.83$)

Discussion

Heating increased and decreased PyOM pH

Our results suggested that subsequent fire both decreased and increased the pH of PyOM, depending on HF and depth, as those factors determined the heat that PyOM received. This was not consistent with our hypothesis that pH would increase consistently with heat exposure, but was similar to the results of the past literature regarding heating soil (samples that are not PyOM-only). Studies have found that low-temperature heating (150 ~ 250 °C) caused pH of soil to decrease (Badía & Martí, 2003; Fernández et al., 1997), and then pH gradually increased until temperatures reached their maximum tested value of 490 °C (Fernández et al., 1997). Our quadratic model predicted 200 °C led to the lowest pH, which was the median of the range in previous research (150 ~ 250 °C), with the lowest pH occurring for treatments High HF + 5cm and Low HF + 1 cm.

Previous soil heating studies have also observed significant pH increases occurring at > 450 °C due to alkaline substances released in fuel combustion or loss of hydroxyl groups in clay (Badía & Martí, 2003; Bárcenas-Moreno et al., 2022; Knicker, 2007). This is also consistent with our results for the treatments High HF + Surface and High HF + 1 cm. Both of these treatments had peak temperatures > 500 °C for all the samples, and pH values for these two treatments were significantly higher than the controls, which might be because of the ash production under the near complete combustion. Finally, when soil was heated to temperatures below 150 °C in other studies, little change was observed in soil properties (Fernández et al., 1997), which is also consistent with our results for the treatment Low HF + 5cm (with peak temperature < 150 °C), which were not significantly different from the controls. While this does not mean chemical transformation were not occurring at these lower temperatures, especially given the fact that PyOM mass and C loss did occur in treatment Low HF + 5cm. Although under different conditions, Cheng et al. (2006)

have shown that high-temperature incubation (70 °C) can significantly increase acidic functional groups, such as carboxylic groups, while the phenolic and lactonic groups originally present in PyC did not increase.

In general, our pH results can be explained by past experiments and also challenge the "common knowledge" that fire always increases pH from ash production. If a full gradient of pH changes with temperature could be measured, we could possibly use such data to estimate the heating temperatures reached at a local scale in the soil profile during a fire.

pH vs. DOC and pH vs. DIC

Besides the differences in pH change across all the treatments, we also saw a negative correlation between pH and DOC (Figure 3.8a), and a positive correlation between pH and DIC (Figure 3.8b). We would assume that higher DOC content may be related to more organic acids produced in lower-temperature heating, which leads to lower pH. On the other hand, DIC, such as carbonate and bicarbonate ions, could associate with the basic cations such as K^+, Ca^{2+}, and Mg^{2+}, which are in high concentration after near-complete combustion (Pellegrini et al., 2018), and cause pH to increase, as shown in treatments High HF + Surface, High HF + 1 cm, and Low HF + Surface. We also found that treatments generating higher DOC content usually correspondingly have lower DIC content and vice versa. This might be due to the enhanced "liming effect" after most organic carbon (OC) is depleted, while when substantial OC remains, it might subdue the liming effect that prevents pH to increase. Wang et al. (2012) used sequential loss on ignition (LOI) methods to measure the content of SOM and DIC. The mass of SOM is inferred from mass loss of dry soil after heating at 375 °C for 17 hours; the DIC is measured by heating the same soil again at 800 °C for 12 hours. Although our heating duration was not as long as 17 hours, it still combusted a major

amount of OC for treatments High HF + Surface, High HF + 1 cm, and Low HF + Surface, which left the DIC abundant enough to cause the increase of pH.

Subsequent fire caused C loss of the preexisting PyOM

Doerr et al. (2018) found that higher fire intensity caused higher mass and PyC losses, and Tinkham et al., (2016) found that less PyC remained after each reburn, which means that we should expect C loss in the PyOM during the reburn and more C loss under high HF. Our results are consistent with that – for all the treatments, we observed C loss and more C loss occurred under high HF when the PyOM was at the same depth (Figure 3.2a). Previous related studies haven't used depth as a variable, although Tinkham et al., (2016) suggested that burial depth > 3 cm in the mineral soil could prevent thermal degradation. However, in our experiment, at the depth of 5 cm, 40.09±1.76% and 2.57±0.60% of total C got lost from High HF and Low HF, respectively (Table S3.9), indicating the interactive effects between exposure depth and heat treatment in estimating the protection of thermal degradation. Regardless, though, C losses should be consistently expected to decrease with depth, with greatest – and in some cases, near-complete – losses at the surface and near surface (Table S3.9). These trends in observed C losses of PyOM were generally consistent with our hypothesis.

Subsequent fire changed PyOM mineralizability

After the 12-week incubation, we found that, relative to controls, more mineralized C and higher mineralizability were observed in treatments High HF + 5 cm and Low HF + 1 cm (mineralizablity was not significantly higher in High HF + 5 cm but showed a higher trend) (Figure 3.3a & b), and less C was mineralized in treatments High HF + Surface, High HF + 1 cm, and Low HF + Surface (Figure 3.3a). Different from our hypothesis that higher heat exposure would lead to

lower mineralized C, we observed higher mineralized C for intermediate heat exposures, which exhibited a different trend from total C remaining (which consistently decreased). For treatment Low HF + Surface, we saw higher mineralizability (or mineralized fraction) on a per-g C basis (Figure 3.3b) although the mineralized C and total C were smaller, due to combustion losses. We also found that the mineralized C fraction (per g of C) was positively related to the modeled degradable C fraction (*a*) (Figure 3.6).The degradation rate (*b*) is also relatively higher in treatments High HF + 5 cm (but not significantly) and Low HF + 1 cm (Figure 3.5b), indicating that the remaining PyOM after reburn may experience fast loss from microbial decomposition in a short period of time. Together, these results underscore that, at certain burial depths and heat treatments, not only are there direct losses of C due to combustion, but the remaining C is even more susceptible to degradation, further exacerbating potential net C losses from subsequent fires. Since there were no previous incubation results in the related studies of reburned PyOM, we also measured DOC to further analyze the chemical properties that influence mineralizability.

Mineralized C was positively correlated with DOC

We found that mineralized C was positively correlated with DOC (Figure 3.9). This positive correlation is consistent with past findings that DOC likely contributes to the labile fraction of the total C that is more preferred and easily decomposed by microbes (Zeba et al., 2023). From this linear correlation, we may estimate that major portions of DOC produced in the fire might be decomposed by microbial mineralization, especially in biologically active sites. C loss as CO_2 from microbial decomposition could persist for years to centuries after a fire (Ascough et al., 2018; Singh et al., 2014). Furthermore, these readily mineralizable fractions may induce positive priming (stimulation of the degradation of the other preexisting organic matter) after the addition of PyOM, further diminishing the effects of PyC on C sequestration tovertime (Dungait

et al., 2012). Without any major disturbance (such as a fire), PyC pools in the top 30 cm of soil typically decline within 100 years after the deposition of PyOM (Foereid et al., 2011) due to mineralization and losses via leaching or erosion. For example, although pine-derived PyC produced from 450 °C can have mean residence times of hundreds of years, which is much slower than that of unburned woody C and soil C, the PyC can still be accessed by many groups of heterotrophic microbial communities (Santos et al., 2012).

DOC indicates PyC mobility, sequestration, and persistence

Although a relatively small fraction of total PyC, DPyC is important due to its mineralizability and also, movability (Santos et al., 2022). Consistent with our results, previous studies have also observed that oxidation from fire increases the water solubility of PyC (Preston & Schmidt, 2006). Other studies have observed more DOC leached from surface soil with lower-temperature heating (300 °C) than with higher temperatures (450 °C) (Santos et al., 2022), which corresponds to our results.

While PyC can be moved into deeper soil horizons over time, the majority stays in the top 30 cm (Silva et al., 2023), with 70 % of that in the top 10 cm (DeLuca & Alpet, 2008). Therefore, DPyC accounts for most of the vertical movement and burial of PyC in the mineral soil (Major et al., 2010; Preston & Schmidt, 2006), where it contributes to total OM stocks in subsoil horizons, in which half of the total C stock is located (Rumpel & Kögel-Knabner, 2011). The release of DPyC could be a long-term process even when fire is absent (Santos et al., 2017). As DPyC can be high in aromaticity, this vertical movement could help explain why stable C tend to increase as depth increases (Boot et al., 2004; Dungait et al., 2012; Hobley, 2019).

Implications for adopting fire in land management

Our results showed that PyOM recombustion is likely to occur under higher fire intensity and when PyOM remains at the surface. Also from previous studies, we could expect that the macroscopic PyC (or residual PyC) theoretically tends to remain in situ after fire (Bird et al., 2015; Tinner et al., 2006). Although it has a bigger particle size, macroscopic C is more susceptible to loss in the subsequent fire because of shallow burial and relatively smaller surface area to host chemical and biological reactions, which prevents macroscopic C from being incorporated into soil by microbes. These findings have implications for fire management. Effective fire management always requires understanding the ecosystem and the original fire regime, while also ensuring the safety of people and properties.

Fire management or fire regime help determine fire severity and fire return interval, which, in turn, influence the effects of subsequent fire on PyOM, through changes in direct combustion losses and transformations, and potential burial depth of PyOM between fires. In general, low-severity fires cause less change in soils (Matosziuk et al., 2019), but may also be associated with more frequent fires, and, hence, shorter time for PyOM burial between fires. Management decisions that lead to increasing tree density may add risks for high-severity fires to occur, especially in the context of climate change (Hermoso et al., 2021), thereby also increasing likelihood of PyC losses through combustion. More soil PyC loss can also be observed after subsequent fires in lower-frequency fire regimes (such as boreal regions) due to the accumulation of forest litter during the long fire return interval (FRI), which can produce ground fire and lead to high soil burn severity. High fire frequency could also potentially consume residual PyC from recombustion and negatively influence long-term accumulation (Preston & Schmidt, 2006).

If the management goal is to increase or maintain soil PyC stocks, fire management should consider the factors that 1) affect HF to soils, including description and observation of fuel loading in the forest (Keane et al., 2012), fuel removal, and controlled burns in small patches; 2) affect PyOM burial, including modeling the typical FRI to give sufficient time for PyOM incorporation. Typically, other goals besides C management drive fire management decisions, such as forest regeneration, land restoration, and fire risk management. Thus, effective communication between different stakeholders is essential to work towards optimizing the common goals.

Conclusion

Based on the results of the full-factorial experiment with different burial depths of PyOM and different heat flux profiles, we conclude that subsequent fires consume residual PyOM while also making the PyOM more susceptible to microbial decomposition. We found that high HF and/or surface fires (High HF + Surface, High HF + 1 cm, and Low HF + Surface) resulted in large direct C losses, which is biggest effect to explain the consumption mechanism of fire. While intermediate HF and/or depth fires (High HF + 5 cm and Low HF + 1 cm) resulted in losses along with increased DOC and mineralizability, which could lead to more complicated long-term effects: increase in the dissolved fraction of PyOM may make it more easily move down in mineral soil and contribute to the persistent C pool in deep soil, and may also make it more easily decomposed by microbes. In the lowest HF / depth fire (Low HF + 5 cm), much PyC was retained, and changes to lability / DOC may be minimal. Moreover, pH, an important chemical property of PyOM, was subject to decreases at low-temperature heating and increases at higher temperatures.

Our experiments expanded the studied changes in chemical and biological properties of PyOM after subsequent fire, building off related studies, especially with the inclusion of the post-reburn incubation. In addition, the laboratory settings were also more controlled compared to other

related studies. Future studies should represent different fire regimes, to provide a holistic view of the impact of repeated fires on the PyC cycle.

Reference

Abiven, S., & Santín, C. (2019). Editorial: From Fires to Oceans: Dynamics of Fire-Derived Organic Matter in Terrestrial and Aquatic Ecosystems. *Frontiers in Earth Science*, *7*, 31. doi: 10.3389/feart.2019.00031

Abney, R. B., & Berhe, A. A. (2018). Pyrogenic Carbon Erosion: Implications for Stock and Persistence of Pyrogenic Carbon in Soil. *Frontiers in Earth Science*, *6*, 26. doi: 10.3389/feart.2018.00026

Allison, S. D., & Vitousek, P. M. (2004). Extracellular Enzyme Activities and Carbon Chemistry as Drivers of Tropical Plant Litter Decomposition. *Biotropica*, *36*(3), 285–296. doi: 10.1111/j.1744-7429.2004.tb00321.x

Ascough, P. L., Bird, M. I., Meredith, W., Snape, C., Large, D., Tilston, E., … Shen, L. (2018). Dynamics of Charcoal Alteration in a Tropical Biome: A Biochar-Based Study. *Frontiers in Earth Science*, *6*, 61. doi: 10.3389/feart.2018.00061

Badía, D., & Martí, C. (2003). Plant Ash and Heat Intensity Effects on Chemicaland Physical Properties of Two Contrasting Soils. *Arid Land Research and Management*, *17*(1), 23–41. doi: 10.1080/15324980301595

Bárcenas-Moreno, G., Jiménez-Compán, E., Emeterio, L. M. S., Jiménez-Morillo, N. T., & González-Pérez, J. A. (2022). Soil pH and Soluble Organic Matter Shifts Exerted by Heating Affect Microbial Response. *International Journal of Environmental Research and Public Health*, *19*(23), 15751. doi: 10.3390/ijerph192315751

Bird, M. I., Wynn, J. G., Saiz, G., Wurster, C. M., & McBeath, A. (2015). The Pyrogenic Carbon Cycle. *Annual Review of Earth and Planetary Sciences*, *43*(1), 1–26. doi: 10.1146/annurev-earth-060614-105038

Boot, C. M., Haddix, M., Paustian, K., & Cotrufo, M. F. (2014). Distribution of black carbon in Ponderosa pine litter and soils following the High Park wildfire. *Biogeoscience Discussions, 12,* 1-11. doi: 10.5194/bgd-11-16799-2014

Cheng, C.-H., Lehmann, J., Thies, J. E., Burton, S. D., & Engelhard, M. H. (2006). Oxidation of black carbon by biotic and abiotic processes. *Organic Geochemistry*, *37*(11), 1477–1488. doi: 10.1016/j.orggeochem.2006.06.022

DeLuca, T. H., & Aplet, G. H. (2008). Charcoal and carbon storage in forest soils of the Rocky Mountain West. *Frontiers in Ecology and the Environment*, *6*(1), 18–24. doi: 10.1890/070070

Ding, Y., Cawley, K. M., Cunha, C. N. da, & Jaffé, R. (2014). Environmental dynamics of dissolved black carbon in wetlands. *Biogeochemistry*, *119*(1–3), 259–273. doi: 10.1007/s10533-014-9964-3

Dittmar, T., Paeng, J., Gihring, T. M., Suryaputra, I. G. N. A., & Huettel, M. (2012). Discharge of dissolved black carbon from a fire-affected intertidal system. *Limnology and Oceanography*, *57*(4), 1171–1181. doi: 10.4319/lo.2012.57.4.1171

Doerr, S. H., Santín, C., Merino, A., Belcher, C. M., & Baxter, G. (2018). Fire as a Removal Mechanism of Pyrogenic Carbon From the Environment: Effects of Fire and Pyrogenic Carbon Characteristics. *Frontiers in Earth Science*, *6*, 127. doi: 10.3389/feart.2018.00127

Dungait, J. A. J., Hopkins, D. W., Gregory, A. S., & Whitmore, A. P. (2012). Soil organic matter turnover is governed by accessibility not recalcitrance. *Global Change Biology*, *18*(6), 1781–1796. doi: 10.1111/j.1365-2486.2012.02665.x

Elzhov TV, Mullen KM, Spiess A, Bolker B (2023). *minpack.lm: R Interface to the Levenberg-Marquardt Nonlinear Least-Squares Algorithm Found in MINPACK, Plus Support for Bounds*. https://CRAN.R-project.org/package=minpack.lm

Fernández, I., Cabaneiro, A., & Carballas, T. (1997). Organic matter changes immediately after a wildfire in an atlantic forest soil and comparison with laboratory soil heating. *Soil Biology and Biochemistry*, *29*(1), 1–11. doi: 10.1016/s0038-0717(96)00289-1

Foereid, B., Lehmann, J., & Major, J. (2011). Modeling black carbon degradation and movement in soil. *Plant and Soil*, *345*(1–2), 223–236. doi: 10.1007/s11104-011-0773-3

Forbes, M. S., Raison, R. J., & Skjemstad, J. O. (2006). Formation, transformation and transport of black carbon (charcoal) in terrestrial and aquatic ecosystems. *Science of The Total Environment*, *370*(1), 190–206. doi: 10.1016/j.scitotenv.2006.06.007

Graves, S., Pipepho, H., Dorai-Raj, S. (2019). *multcompView: Visualizations of Paired Comparisons*. https://CRAN.R-project.org/package=multcompView

Hermoso, V., Regos, A., Morán-Ordóñez, A., Duane, A., & Brotons, L. (2021). Tree planting: A double-edged sword to fight climate change in an era of megafires. *Global Change Biology*, *27*(13), 3001–3003. doi: 10.1111/gcb.15625

Hobley, E. (2019). Vertical Distribution of Soil Pyrogenic Matter: A Review. *Pedosphere*, *29*(2), 137–149. doi: 10.1016/s1002-0160(19)60795-2

Hofmann, D., Steffen, D., Jablonowski, N. D., & Burauel, P. (2012). *Dissolved organic carbon (DOC) in soil extracts investigated by FT-ICR-MS*. 13957. Retrieved from ui.adsabs.harvard.edu/abs/2012EGUGA..1413957H/abstract

Johnson, D. B., Woolet, J., Yedinak, K. M., & Whitman, T. (2023). Experimentally determined traits shape bacterial community composition one and five years following wildfire. *Nature Ecology & Evolution*, 1–13. doi: 10.1038/s41559-023-02135-4

Jones, D. L., & Willett, V. B. (2006). Experimental evaluation of methods to quantify dissolved organic nitrogen (DON) and dissolved organic carbon (DOC) in soil. *Soil Biology and Biochemistry*, *38*(5), 991–999. doi: 10.1016/j.soilbio.2005.08.012

Keane, R. E. (2012). Describing wildland surface fuel loading for fire management: a review of approaches, methods and systems. *International Journal of Wildland Fire*, *22*(1), 51–62. doi: 10.1071/wf11139

Knicker, H. (2007). How does fire affect the nature and stability of soil organic nitrogen and carbon? A review. *Biogeochemistry*, *85*(1), 91–118. doi: 10.1007/s10533-007-9104-4

Knicker, H. (2011). Pyrogenic organic matter in soil: Its origin and occurrence, its chemistry and survival in soil environments. *Quaternary International*, *243*(2), 251–263. doi: 10.1016/j.quaint.2011.02.037

Major, J., Lehmann, J., Rondon, M., & Goodale, C. (2010). Fate of soil-applied black carbon: downward migration, leaching and soil respiration. *Global Change Biology*, *16*(4), 1366–1379. doi: 10.1111/j.1365-2486.2009.02044.x

Matosziuk, L. M., Alleau, Y., Kerns, B. K., Bailey, J., Johnson, M. G., & Hatten, J. A. (2019). Effects of season and interval of prescribed burns on pyrogenic carbon in ponderosa pine stands in the southern Blue Mountains, Oregon, USA. *Geoderma*, *348*, 1–11. doi: 10.1016/j.geoderma.2019.04.009

Ohlson, M., Dahlberg, B., Økland, T., Brown, K. J., & Halvorsen, R. (2009). The charcoal carbon pool in boreal forest soils. *Nature Geoscience*, *2*(10), 692–695. doi: 10.1038/ngeo617

Oksanen J., Simpson G., Blanchet F., Kindt R., Legendre P., …, Weedon J. (2022). *vegan: Community Ecology Package*. https://CRAN.R-project.org/package=vegan

Pellegrini, A. F. A., Ahlström, A., Hobbie, S. E., Reich, P. B., Nieradzik, L. P., Staver, A. C., … Jackson, R. B. (2018). Fire frequency drives decadal changes in soil carbon and nitrogen and ecosystem productivity. *Nature*, *553*(7687), 194–198. doi: 10.1038/nature24668

Pingree, M. R. A., & DeLuca, T. H. (2017). Function of Wildfire-Deposited Pyrogenic Carbon in Terrestrial Ecosystems. *Frontiers in Environmental Science*, *5*, 53. doi: 10.3389/fenvs.2017.00053

Preston, C. M., & Schmidt, M. W. I. (2006). Black (pyrogenic) carbon: a synthesis of current knowledge and uncertainties with special consideration of boreal regions. *Biogeosciences*, *3*(4), 397–420. doi: 10.5194/bg-3-397-2006

R Core Team (2022*). R: language and environment for statistical computing. R Foundation for Statistical Computing, Vienna, Austria. URL https://www.R-project.org/.*

Rumpel, C., & Kögel-Knabner, I. (2011). Deep soil organic matter—a key but poorly understood component of terrestrial C cycle. *Plant and Soil*, *338*(1–2), 143–158. doi: 10.1007/s11104-010-0391-5

Santín, C., Doerr, S. H., Kane, E. S., Masiello, C. A., Ohlson, M., Rosa, J. M., … Dittmar, T. (2016). Towards a global assessment of pyrogenic carbon from vegetation fires. *Global Change Biology*, *22*(1), 76–91. doi: 10.1111/gcb.12985

Santín, C., Doerr, S. H., Preston, C., & Bryant, R. (2013). Consumption of residual pyrogenic carbon by wildfire. *International Journal of Wildland Fire*, *22*(8), 1072–1077. doi: 10.1071/wf12190

Santos, F., Bird, J. A., & Berhe, A. A. (2022). Dissolved pyrogenic carbon leaching in soil: Effects of soil depth and pyrolysis temperature. *Geoderma*, *424*, 116011. doi: 10.1016/j.geoderma.2022.116011

Santos, F., Torn, M. S., & Bird, J. A. (2012). Biological degradation of pyrogenic organic matter in temperate forest soils. *Soil Biology and Biochemistry*, *51*, 115–124. doi: 10.1016/j.soilbio.2012.04.005

Santos, F., Wagner, S., Rothstein, D., Jaffe, R., & Miesel, J. R. (2017). Impact of a Historical Fire Event on Pyrogenic Carbon Stocks and Dissolved Pyrogenic Carbon in Spodosols in Northern Michigan. *Frontiers in Earth Science*, *5*, 80. doi: 10.3389/feart.2017.00080

Schindelbeck, R., Moebius-Clune, D., Kurtz, K., van Es, H. M., Gugino, B., Idowu, O., ... & Abawi, G. S. (2016). Cornell soil health laboratory comprehensive assessment of soil health standard operating procedures February 2016.

Silva, L. J. da, Oliveira, D. M. da S., Nóbrega, G. N., Barbosa, R. I., & Cordeiro, R. C. (2023). Pyrogenic carbon stocks and its spatial variability in soils from savanna-forest ecotone in amazon. *Journal of Environmental Management*, *340*, 117980. doi: 10.1016/j.jenvman.2023.117980

Singh, N., Abiven, S., Maestrini, B., Bird, J. A., Torn, M. S., & Schmidt, M. W. I. (2014). Transformation and stabilization of pyrogenic organic matter in a temperate forest field experiment. *Global Change Biology*, *20*(5), 1629–1642. doi: 10.1111/gcb.12459

Singh, N., Abiven, S., Torn, M. S., & Schmidt, M. W. I. (2012). Fire-derived organic carbon in soil turns over on a centennial scale. *Biogeosciences*, *9*(8), 2847–2857. doi: 10.5194/bg-9-2847-2012

Sokol, N. W., Slessarev, E., Marschmann, G. L., Nicolas, A., Blazewicz, S. J., Brodie, E. L., … Pett-Ridge, J. (2022). Life and death in the soil microbiome: how ecological processes influence biogeochemistry. *Nature Reviews Microbiology*, *20*(7), 415–430. doi: 10.1038/s41579-022-00695-z

Strotmann, U., Reuschenbach, P., Schwarz, H., & Pagga, U. (2004). Development and evaluation of an online CO(2) evolution test and a multicomponent biodegradation test system. *Applied and environmental microbiology*, *70*(8), 4621–4628. https://doi.org/10.1128/AEM.70.8.4621-4628.2004

Tinkham, W. T., Smith, A. M. S., Higuera, P. E., Hatten, J. A., Brewer, N. W., & Doerr, S. H. (2016). Replacing time with space: using laboratory fires to explore the effects of repeated burning on black carbon degradation. *International Journal of Wildland Fire*, *25*(2), 242–248. doi: 10.1071/wf15131

Tinner, W., Hofstetter, S., Zeugin, F., Conedera, M., Wohlgemuth, T., Zimmermann, L., & Zweifel, R. (2006). Long-distance transport of macroscopic charcoal by an intensive crown fire in the Swiss Alps - implications for fire history reconstruction. *The Holocene*, *16*(2), 287–292. doi: 10.1191/0959683606hl925rr

Tukey, J. W. (1949). Comparing Individual Means in the Analysis of Variance. *Biometrics*, *5*(2), 99. doi: 10.2307/3001913

Wang, X., Wang, J., & Zhang, J. (2012). Comparisons of Three Methods for Organic and Inorganic Carbon in Calcareous Soils of Northwestern China. *PLoS ONE*, *7*(8), e44334. doi: 10.1371/journal.pone.0044334

Wickham, H. (2016). *ggplot2: Elegant Graphics for Data Analysis*. Springer-Verlag New York. ISBN 978-3-319-24277-4, https://ggplot2.tidyverse.org.

Wickham H, François R, Henry L, Müller K (2022). *dplyr: A Grammar of Data Manipulation_*. https://CRAN.R-project.org/package=dplyr.

Whitman, T., Hanley, K., Enders, A., & Lehmann, J. (2013). Predicting pyrogenic organic matter mineralization from its initial properties and implications for carbon management. *Organic Geochemistry*, *64*, 76–83. doi: 10.1016/j.orggeochem.2013.09.006

Whitman, T., Zhu, Z., & Lehmann, J. (2014). Carbon Mineralizability Determines Interactive Effects on Mineralization of Pyrogenic Organic Matter and Soil Organic Carbon. *Environmental Science & Technology*, *48*(23), 13727–13734. doi: 10.1021/es503331y

Zeba, N., Berry, T. D., Panke-Buisse, K., & Whitman, T. (2022). Effects of physical, chemical, and biological ageing on the mineralization of pine wood biochar by a Streptomyces isolate. *PLoS ONE*, *17*(4), e0265663. doi: 10.1371/journal.pone.0265663

Zeba, N., Berry, T. D., Fischer, M. S., Traxler, M. F., & Whitman, T. (2023). Soil carbon mineralization and microbial community dynamics in response to PyOM addition. doi: 10.1101/2023.06.21.545992

Supplementary Information (Chapter 3)

Table S3.1. ANOVA statistics for pH

Sources	df	Sum of Squares	Mean Squares	F statistic	p-value
Heat Flux	2	0.8646	0.4323	51.86	$< 2.51 \cdot 10^{-11}$
Depth	2	0.7301	0.3651	43.79	$< 2.28 \cdot 10^{-10}$
Heat Flux · Depth	4	2.0824	0.5206	62.45	$< 1.07 \cdot 10^{-15}$
Residuals	36	0.3001	0.0083		

Table S3.2. ANOVA statistics for total C (%)

Sources	df	Sum of Squares	Mean Squares	F statistic	p-value
Heat Flux	2	4.493	2.2463	8510	$< 2 \cdot 10^{-16}$
Depth	2	1.937	0.9686	3670	$< 2 \cdot 10^{-16}$
Heat Flux · Depth	4	1.096	0.2740	1038	$< 2 \cdot 10^{-16}$
Residuals	36	0.010	0.0003		

Table S3.3. ANOVA statistics for CO_2-C (g)

Sources	df	Sum of Squares	Mean Squares	F statistic	p-value
Heat Flux	2	$2.620 \cdot 10^{-7}$	$1.312 \cdot 10^{-7}$	7.401	0.00209
Depth	2	$2.451 \cdot 10^{-6}$	$1.225 \cdot 10^{-6}$	69.112	$7.01 \cdot 10^{-13}$
Heat Flux · Depth	4	$5.348 \cdot 10^{-6}$	$1.337 \cdot 10^{-6}$	75.404	$< 2 \cdot 10^{-16}$
Residuals	35	$6.210 \cdot 10^{-7}$	$1.770 \cdot 10^{-8}$		

Table S3.4. ANOVA statistics for C mineralizability (g CO_2-C · g^{-1} C)

Sources	df	Sum of Squares	Mean Squares	F statistic	p-value
Treatments	6	0.0013717	$2.286 \cdot 10^{-4}$	8.327	$3.16 \cdot 10^{-5}$
Residuals	28	0.0007688	$2.746 \cdot 10^{-5}$		

Table S3.5. ANOVA statistics for degradable C fraction

Sources	df	Sum of Squares	Mean Squares	F statistic	p-value
Treatments	6	0.0027905	0.0004651	37.97	$6.31 \cdot 10^{-12}$
Residuals	27	0.0003307	0.0000122		

Table S3.6. ANOVA statistics for C degradation rate ($week^{-1}$)

Sources	df	Sum of Squares	Mean Squares	F statistic	p-value
Treatments	6	0.08787	0.014645	6.645	0.000211
Residuals	27	0.05950	0.002204		

Table S3.7. ANOVA statistics for DOC (mg C · g^{-1} sample)

Sources	df	Sum of Squares	Mean Squares	F statistic	p-value
Heat Flux	2	0.002993	0.0014963	62.90	$1.79 \cdot 10^{-12}$
Depth	2	0.004873	0.0024363	102.41	$1.39 \cdot 10^{-15}$
Heat Flux · Depth	4	0.008983	0.0022456	94.39	$< 2 \cdot 10^{-16}$
Residuals	36	0.000856	0.0000238		

Table S3.8. ANOVA statistics for DIC (mg C · g^{-1} sample)

Sources	df	Sum of Squares	Mean Squares	F statistic	p-value
Heat Flux	2	$5.420 \cdot 10^{-6}$	$2.710 \cdot 10^{-6}$	5.60	0.00763
Depth	2	$8.250 \cdot 10^{-5}$	$4.125 \cdot 10^{-5}$	85.23	$2.22 \cdot 10^{-14}$
Heat Flux · Depth	4	$9.989 \cdot 10^{-5}$	$2.497 \cdot 10^{-5}$	51.59	$2.02 \cdot 10^{-14}$
Residuals	36	$1.742 \cdot 10^{-5}$	$4.800 \cdot 10^{-7}$		

Table S3.9. C loss fraction for all treatments (n = 5; controls not included); Different superscript letters (ANOVA, Tukey's HSD) indicate significant differences across all treatments

Heat Flux	**Depth**	**C Loss Fraction (%)**	**SD (%)**
High	Surface	99.05^{a}	0.16
High	1cm	99.05^{a}	0.13
High	5cm	40.09^{d}	1.76
Low	Surface	91.78^{b}	0.69
Low	1cm	53.22^{c}	3.37
Low	5cm	2.57^{e}	0.60

Conclusion and Outlook

Given the history of using fire as a land management tool and naturally fire-dependent ecosystems, we should view fire as more of an ecological process and not simply as a hazard. With this change in view in recent years, the fire regime of some areas of North America has been planned to be restored to pre-European settlement conditions. However, due to the hotter and drier fire seasons caused by climate change, as well as excessive fuel accumulation, we still expect to see high severity and frequent wildfires in many areas in the near future. Pyrogenic organic matter (PyOM) and pyrogenic carbon (PyC) that remain in the location where they were deposited may be subjected to being combusted during subsequent fires. To understand the net effects of reburn on the preexisting PyOM, we applied laboratory burn trials with a full-factorial design to test how different heat flux (HF) profiles (High HF, Low HF, Control) and exposure depths (Surface, 1 cm, and 5 cm) influence the physical, chemical, and biological properties of PyOM.

We parameterized realistic HF profiles using log burns and applied the HF profiles to PyOM using a cone calorimeter as a simulation of reburns on the forest floor. This method for HF stimulation was highly replicable and provided distinctive temperature profiles and heat exposures for each treatment, which could be adopted for further soil heating experiments.

The most related laboratory PyOM-reburn studies have either only targeted mass loss of PyOM (Bartoli et al., 2021; Saiz et al., 2014; Santín et al., 2013) or have conducted experiments only focusing on the chemical properties of PyOM (Doerr et. al., 2018; Tinkham et al., 2016). Experiments for studying soil PyOM and PyC in other contexts also emphasize chemical recalcitrance and aromaticity from the adoption of a variety of oxidation methods, such as CTOs and BPCA (Roth et al., 2012). Those methods could underestimate actual PyC stocks because they overlook PyC fractions with lower stability, particularly that produced during heat oxidation.

Instead, we targeted PyC fractions with lower persistence by using incubations and DOC measurement, recognizing that soil organic matter (SOM) turnover is governed by accessibility in addition to chemical structure (Dungait et al., 2012).

Our results showed that subsequent fire not only combusted PyOM *in situ* (especially under higher heat fluxes and when PyOM remains at the surface), but also made PyOM more susceptible to post-fire microbial decomposition. This indicated that PyOM produced in natural fire is different from PyOM intentionally produced during pyrolysis (such as biochar). In oxygen-limited environments, higher temperatures can lead to higher aromaticity and less labile fractions (Ascough et al., 2011). Increasing temperatures during low-oxygen heating can reduce carboxyl and hydroxyl groups and form more persistent aromatic structures (Pingree & DeLuca, 2017). However, this mechanism does not occur in aerobic environments, as we simulated here. With the presence of oxygen, high temperatures no longer condense PyOM to a more recalcitrant form, but, rather, simply combust much of it. Low-temperature heating of near-surface soil could also increase the soluble fraction of PyOM, making it more easily migrate into mineral soil and contribute to the stable C pool in deep soil over time; however, this represents a relatively small fraction of total PyC, and it is also subject to being eroded out of the system. The effects of fire on C stocks should be re-evaluated from multiple perspectives because pathways of PyOM movement during fire return intervals are complicated.

Moreover, fire in nature is more complicated than fire generated in all laboratorial settings (like cone calorimeter and muffle furnace). For example, high-intensity crown fire, which is typical in boreal forests, could char the aboveground biomass, but may not cause severe soil C loss. A higher amount of PyOM and higher C concentration are observed in a higher percentage of burned boreal forest ground (Ohlson et al., 2009), which is more likely in the northernmost jack pine

barren in Wisconsin with stand-replacing fire. However, low-intensity ground fire can lead to severe oxidation of soil C even though the ground fire in nature is considered oxygen-limited (Bryant et al., 2013), which may be observed in the more southern part of the pine barren with higher fire frequency (Radeloff et al., 2004).

We also found that increasing heat exposure can cause the pH of PyOM to decrease at first at lower temperatures and then increase at higher temperatures. Future work may consider the exact chemical process at work in this process.

Our burn unit with quartz sand provided a controlled laboratory setting and ensured the PyOM was the only carbon input, however, it hindered us in performing more analyses of the physical properties of PyOM, such as hydrophobicity, particle size analysis, and density, because we homogenized the residual PyOM and sand after the burn for the complete collection of PyOM while we found it difficult to separate PyOM only.

In future work, we hope to expand our system with the addition of PyOM produced at 550 °C, representing more aromatic PyC and applying more than one subsequent fire to the system with different combinations of sequence for high and low-intensity fires. We also seek to compare the fire regime of Wisconsin pine barrens to other systems, such as prairie fires, and observe the effects of subsequent fire on PyOM in different ecosystems.

Reference

Ascough, P. L., Bird, M. I., Francis, S. M., Thornton, B., Midwood, A. J., Scott, A. C., & Apperley, D. (2011). Variability in oxidative degradation of charcoal: Influence of production conditions and environmental exposure. *Geochimica et Cosmochimica Acta, 75*(9), 2361–2378. doi: 10.1016/j.gca.2011.02.002

Bartoli, F., Foderi, C., & Mastrolonardo, G. (2021). Effect of repeated burnings, fire and charcoal characteristics on natural charcoal re-combustion in a Mediterranean environment as evaluated in laboratory burning experiments. *Geoderma, 402*, 115331. doi: 10.1016/j.geoderma.2021.115331

Bryant, R., Doerr, S. H., & Helbig, M. (2005). Effect of oxygen deprivation on soil hydrophobicity during heating. *International Journal of Wildland Fire, 14*(4), 449–455. doi: 10.1071/wf05035

Doerr, S. H., Santín, C., Merino, A., Belcher, C. M., & Baxter, G. (2018). Fire as a Removal Mechanism of Pyrogenic Carbon From the Environment: Effects of Fire and Pyrogenic Carbon Characteristics. *Frontiers in Earth Science, 6*, 127. doi: 10.3389/feart.2018.00127

Dungait, J. A. J., Hopkins, D. W., Gregory, A. S., & Whitmore, A. P. (2012). Soil organic matter turnover is governed by accessibility not recalcitrance. *Global Change Biology, 18*(6), 1781–1796. doi: 10.1111/j.1365-2486.2012.02665.x

Ohlson, M., Dahlberg, B., Økland, T., Brown, K. J., & Halvorsen, R. (2009). The charcoal carbon pool in boreal forest soils. *Nature Geoscience, 2*(10), 692–695. doi: 10.1038/ngeo617

Pingree, M. R. A., & DeLuca, T. H. (2017). Function of Wildfire-Deposited Pyrogenic Carbon in Terrestrial Ecosystems. *Frontiers in Environmental Science, 5*, 53. doi: 10.3389/fenvs.2017.00053

Radeloff, V. C., Mladenoff, D. J., Guries, R. P., & Boyce, M. S. (2004). Spatial patterns of cone serotiny in Pinus banksiana in relation to fire disturbance. *Forest Ecology and Management*, *189*(1–3), 133–141. doi: 10.1016/j.foreco.2003.07.040

Roth, P. J., Lehndorff, E., Brodowski, S., Bornemann, L., Sanchez-García, L., Gustafsson, Ö., & Amelung, W. (2012). Differentiation of charcoal, soot and diagenetic carbon in soil: Method comparison and perspectives. *Organic Geochemistry, 46,* 66–75. doi: 10.1016/j.orggeochem.2012.01.012

Saiz, G., Goodrick, I., Wurster, C. M., Zimmermann, M., Nelson, P. N., & Bird, M. I. (2014). Charcoal re-combustion efficiency in tropical savannas. *Geoderma, 219*, 40–45. doi: 10.1016/j.geoderma.2013.12.019

Santín, C., Doerr, S. H., Preston, C., & Bryant, R. (2013). Consumption of residual pyrogenic carbon by wildfire. *International Journal of Wildland Fire, 22*(8), 1072–1077. doi: 10.1071/wf12190

Tinkham, W. T., Smith, A. M. S., Higuera, P. E., Hatten, J. A., Brewer, N. W., & Doerr, S. H. (2016). Replacing time with space: using laboratory fires to explore the effects of repeated burning on black carbon degradation. *International Journal of Wildland Fire, 25*(2), 242–248. doi: 10.1071/wf15131